Thesis for the Degree of Doctor of Korean Medicine

Vanillic acid attenuates obesity *via* activation of the AMPK pathway and thermogenic factors *in vivo* and *in vitro*

Yunu Jung

Department of Science in Korean Medicine

Graduate School

Kyung Hee University

Seoul, Korea

August, 2018

Vanillic acid attenuates obesity *via* activation of the AMPK pathway and thermogenic factors *in vivo* and *in vitro*

Yunu Jung

Department of Science in Korean Medicine

Graduate School

Kyung Hee University

Seoul, Korea

August, 2018

Vanillic acid attenuates obesity *via* activation of the AMPK pathway and thermogenic factors *in vivo* and *in vitro*

By

Yunu Jung

Advised by

Prof. Jae-Young Um, Ph.D.

Submitted to the Department of Science in Korean Medicine

And the Faculty of the Graduate School of

Kyung Hee University in Partial Fulfilment

of the Requirements for the Degree of

Doctor of Philosophy

Dissertation Committee:

Chairman	Yong Seek Park, Ph.D.
	Kwang Seok Ahn, Ph.D.
	Woong Mo Yang, K.M.D., Ph.D.
	Seong-Kyu Choe, Ph.D.
	Jae-Young Um, Ph.D.

Contents

List of Tables

List of Figures

Abbreviations

ACC, acetyl-CoA carboxylase;

ALT, alanine transaminase;

AMPKα, AMP-activated protein kinase alpha;

AST, aspartate aminotransferase;

BAT, brown adipose tissue;

CaMKIIβ, Ca^{2+}/calmodulin-dependent kinase II beta;

C/EBPα**,** CCAAT/enhancer-binding protein alpha;

CYTO C, CYTOCROME C;

EGCG, epigallocatechin gallate;

eWAT, epididymal WAT;

FA, fatty acid; GAPDH, glyceraldehyde-3-phosphate dehydrogenase;

GLUCO, glucose;

GW, GW9662;

H&E, hematoxylin and eosin;

HFD, high-fat diet;

iWAT, inguinal WAT;

LDL, low-density lipoprotein cholesterol;

LKB1, liver kinase B1;

ND, normal diet;

PGC1α, peroxisome proliferator activated receptor gamma-coactivator 1 alpha;

PPARγ**,** peroxisome proliferator activated receptor gamma;

TC, total cholesterol;

TRO, troglitazone;

UCP1, uncoupling protein 1;

VA, vanillic acid;

WT, wild type

ABSTRACT

Vanillic acid attenuates obesity *via* activation of the AMPK pathway and thermogenic factors *in vivo* and *in vitro*

By Yunu Jung

Advised by Prof. Jae-Young Um

Energy expenditure is a target gaining recent interest for obesity treatment. The anti-obesity effect of vanillic acid (VA), a well-known flavoring agent, was investigated *in vivo* and *in vitro*. High-fat diet (HFD)-induced obese mice and genetically obese *db/db* mice showed significantly decreased body weights by VA administration. The major adipogenic markers, peroxisome proliferator activated receptor gamma (PPARγ) and CCAAT/enhancer-binding protein alpha (C/EBPα), were reduced while the key factor of energy metabolism AMP-activated protein kinase alpha (AMPKα) was increased in the white adipose tissue (WAT) and liver tissue of the VA group mice. Furthermore, VA inhibited lipid accumulation and reduced hepatotoxic/inflammatory markers in liver tissues of mice and HepG2 hepatocytes. VA treatment also decreased differentiation of 3T3-L1 adipocytes by regulating adipogenic factors including PPARγ and C/EBPα. AMPKα siRNA was used to examine whether AMPK was associated with the actions of VA. In AMPKα-nulled 3T3-L1 cells, the inhibition action of VA on PPARγ and C/EBPα was attenuated. Furthermore, in brown adipose tissues of mice and primary cultured brown adipocytes, VA increased mitochondria- and thermogenesis-related factors such as uncoupling protein 1 and PPARγ-coactivator 1 alpha (PGC1α). Taken together, our results suggest that VA has potential as an AMPKα- and thermogenesis-activating anti-obesity agent.

Keywords: vanillic acid; obesity; adipogenesis; thermogenesis; AMP-activated protein kinase alpha

I. INTRODUCTION

Obesity is the cause of many health-related problems. Excessive increase in weight increases the incidence of hepatic steatosis, type 2 diabetes, inflammation and various types of cancer (1, 2). The obesity epidemic has steadily increased in recent years. Approximately 70% of American adults are overweight or obese with a BMI > 25. As a result, the quality of life is decreasing while morbidity and economic damages are increasing (3, 4).

Adipogenesis is known to be related to the etiologies of obesity and other obesity-related metabolic disorders (5). In mammals, adipocytes are divided into 2 types, white and brown, which have opposite functions. White adipocytes store excess energy in the form of triglycerides (TG), while brown adipocytes release energy through thermogenesis. During the process of adipogenesis in 3T3-L1 adipocytes, peroxisome proliferator activated receptor γ (PPARγ) and CCAAT/enhancer-binding protein α (C/EBPα) have key roles as major transcription factors (6). On the other hand, brown adipose tissue (BAT) expresses the brown fat specific mitochondrial uncoupling protein 1 (UCP1) to induce adaptive thermogenesis. Peroxisome proliferator activated receptor coactivator 1-α (PGC1 α), a coactivator to a number of transcription factors, is also an important factor in the action of BAT because it regulates mitochondrial biogenesis (7).

Lipogenesis is an important mechanism for fat accumulation. One of the most important causes of liver fat. Accumulation is the inhibition of AMPK (8). AMPK is an enzyme that acts as an energy homeostasis maintainer in cells. AMPK is involved in the energy metabolism of organs including liver, muscle, and fat tissue (9). Liver kinase B1 (LKB1) and Ca^{2+}/calmodulin-dependent kinase II ß are upstream kinases of AMPK (10, 11). Activation of AMPK causes phosphorylation of the enzyme acetyl-CoA carboxylase (ACC) (12, 13). The ACC enzyme for synthesizing malonyl-CoA is an important precursor in fatty acid (FA) synthesis as it potentially inhibits FA oxidation in mitochondria (14). To study in detail the mechanisms of hepatic steatosis, a cellular hepatic model was previously established by treating human HepG2 cells with free fatty acids (FFAs) (15, 16) including palmitic acid and oleic acid, the main FAs in the human body (17).

Vanillic acid (VA; 4-hydroxy-3-methoxybenzoic acid) is derived from dihydroxybenzoic acid, an oxidized form of vanillin (18). VA is found in high quantities in the root of *Angelica sinensis* (19). VA is also a constituent of wine, vinegar, and argan oil (20). It has antioxidant, antiinflammatory, and anticancer pharmacologic properties (21, 22). A study

by Hsu and Yen (23) showed that VA caused inhibition of intracellular TG in 3T3-L1 adipocytes. However, the antiobese features of VA *in vivo* has not been confirmed; nor has its action on BAT. The purpose of this study was to examine the antiobesity and thermogenic activity of VA and confirm the mechanisms regarding the AMPK pathway in *vivo* and *vitro*.

II. MATERIALS AND METHODS

1. Reagents

DMEM, penicillin–streptomycin, and fetal bovine serum were purchased from Thermo Fisher Scientific (Waltham, MA, USA). VA, insulin, 3-isobutylmethylxanthine, dexamethasone, indomethacin, 3,3,5-triiodo-L-thyronine, and Oil Red O powder were purchased from Sigma-Aldrich (St. Louis,MO, USA).

2. Ethics statement

All procedures in the animal experiments were performed according to and after receiving approval from the Animal Care and Use Committee of the institutional review board of Kyung Hee University [KHUASP (SE)-13-012].

3. Animal experiments

Male C57BL/6J mice (4-week-old), male 5-week-old *Lepr*$^{-/-}$ (*db/db*) mice and age matched wild type (WT) heterozygous mice were purchased from Daehan Biolink Co. (Eumsung, Korea) and maintained for 1 week prior to the experiments. To induce obesity in the C57BL/6J mice, they were fed a HFD (Rodent diet D12492, Research diet, New Brunswick, NJ, USA) consisting of 60% fat for 4 weeks before administrating VA (10, 100 and 1000 mg·kg^{-1}·day^{-1}) or epigallocatechin gallate (EGCG) (20 mg·kg^{-1}·day^{-1}), which is a compound from green tea extract used as a positive control. The mice were then randomly divided into five groups (n = 5 per group): a HFD, a HFD plus 10 mg·kg^{-1}·day^{-1} VA, a HFD plus 100 mg·kg^{-1}·day^{-1} VA, a HFD plus 1,000 mg·kg^{-1}·day^{-1} VA and a HFD plus EGCG group. EGCG was used as a positive control due to its well-known anti-obese features (24). An additional 6-week-administration experiment was done with these three groups and a normal control group which was fed a normal diet.

The *db/db* mice were provided with a laboratory diet and water *ad libitum*. Healthy mice were randomly allocated into three groups as follows (n = 5 per group): a WT group, a *db/db* group, and a *db/db* group administered VA. The control groups (WT and *db/db* group) were orally administered distilled water, while the experiment group was orally administered VA prepared in distilled water (100 mg·kg^{-1} of body weight) five times per week for 4 weeks.

Body weight and food intake of the mice were measured three times per week. At the end of the experiment, the animals were anesthetized under CO_2 asphyxiation, and serum was separated immediately after blood collection via cardiac puncture. The tissues were collected and stored at -80℃.

4. Blood serum analysis

The serum total cholesterol (TC), low-density lipoprotein cholesterol (LDL), high alanine density lipoprotein cholesterol (HDL), triglyceride, alanine transaminase (ALT), aspartate aminotransferase (AST), FFA and glucose (GLUCO) were analyzed using enzymatic colorimetric methods by Seoul Medical Science Institute (Seoul Clinical Laboratories, Seoul, Korea).

5. Histological studies

Hematoxylin and eosin (H&E) staining was done as previously described (25). Microscopic examinations were performed, and photographs were taken under a regular light microscope.

6. Cell isolation, culture and adipocyte differentiation

Brown preadipocytes were obtained from the interscapular BAT of mice (age, post-natal days 1-3), isolated using the method from Klein *et al* (26). Cell culture and differentiation of HepG2 (27), 3T3-L1 cells and primary cultured brown adipocytes (25) were performed as described previously.

7. Cell cytotoxicity assay

Cell viability was measured with a Cell Proliferation MTS kit (Promega Co., Maddison, WI, USA) as previously described (28).

8. Oil Red-O staining

Intracellular lipid accumulation was measured by Oil Red-O staining as previously described (29).

9. RNA isolation and real-time reverse transcription-PCR

Total RNA extraction, cDNA synthesis, and real-time RT-PCR analyses were performed as previously described (28). The primers used in the experiments are listed in Table 1.

Table 1. Primer sequence for real-time quantitative PCR (qPCR) analysis

Target gene	Primer sequences	
Pparg	5′-TGCCAGTACTGCCGTTTTCA-3′ (sense)	5′-GCGAATTGCATTGTGTGACAT-3′ (antisense)
Cebpa	5′-GCCGAGATAAAGCCAAACAA-3′ (sense)	5′-CCTTGACCAAGGAGCTCTCA-3′ (antisense)
AdipoQ	5′-AGACCTGGCCACTTTCTCCTCATT-3′ (sense)	5′-AGAGGAACAGGAGAGCTTGCAACA-3′ (antisense)
Retn	5′-TTCCTTGTCCCTGAACTGCT-3′ (sense)	5′-AGCTCAAGACTGCTGTGCCT-3′ (antisense)
Fabp4	5′-CGTAAATGGGGATTTGGTCA-3′ (sense)	5′-TCGACTTTCCATCCCACTTC-3′ (antisense)
Lipin1	5′-TTCCTTGTCCCTGAACTGCT-3′ (sense)	5′-TGAAGACTCGCTGTGAATGG-3′ (antisense)
Ucp1	5′-AACTGTACAGCGGTCTGCCT-3′ (sense)	5′-TAAGCCGGCTGAGATCTTGT-3′ (antisense)
Ppargc1a	5′-AATGCAGCGGTCTTAGCACT-3′ (sense)	5′-TGTTGACAAATGCTCTTCGC -3′ (antisense)
Sirt3	5′-TCGAAGGAAAGATGTGGTCC-3′ (sense)	5′-ATCTGTCCTGTCCATCCAGC-3′ (antisense)
Cyc	5′-TTGTTCAGAAGTGTGCCCAG-3′ (sense)	5′-CCAGGTGATGCCTTTGTTCT-3′ (antisense)
Gapdh	5′-AACTTTGGCATTGTGGAAGG-3′ (sense)	5′-GGATGCAGGGATGATGTTCT-3′ (antisense)
Srebp1c	5′-ACA CAG CAA GGT GCT GGA G-3′ (sense)	5′-CCA CTA AGG TGC CTA CAG AGC-3′ (antisense)
Fasn	5′-AAC GTC ACT TCC AGC TAG AC-3′ (sense)	5′-GTC CAG GCT GTG GTG ACT CT-3′ (antisense).
Scd1	5′-CCG GAG ACC CTT AGA TCG A-3′ (sense)	5′-TAG CCT GTA AAA GAT TTC TGC AAA CC-3′ (antisense)
Nrf1	5′- CCA CGT TGG ATG AGT ACA CG -3′ (sense)	5′- CAG ACT CGA GGT CTT CCA GG -3′ (antisense)
Nrf2	5′-CCG GAG ACC CTT AGA TCG A-3′ (sense)	5′-TAG CCT GTA AAA GAT TTC TGC AAA CC-3′ (antisense)
Atp5a1	5′-CTGTACTGCATCTACGTCGCGA -3′ (sense)	5′-AGCCTGCTTGGATAGATCGTCATA -3′ (antisense)
Cpt1a	5′-GACTCCGCTCGCTCATTCC -3′ (sense)	5′-GACTGTGAACTGGAAGGCCA -3′ (antisense)
Acadm	5′-ACTCGAAAGCGGCTCACAA -3′ (sense)	5′-ACGGGGATAATCTCCTCTCTGG -3′ (antisense)
Ppargc1b	5′-CGTATTTGAGGACAGCAGCA -3′ (sense)	5′-TACTGGGTGGGCTCTGGTAG -3′ (antisense)
Hsl	5′-CTGAGATTGAGGTGCTGTCG -3′ (sense)	5′-CAAGGGAGGTGAGATGGTAAC -3′ (antisense)
Atgl	5′-ATATCCCACTTTAGCTCCAAGG -3′ (sense)	5′-CAAGTTGTCTGAAATGCCGC -3′ (antisense)

10. Western blot analysis

Western blot analyses were performed as previously described (30). The antibodies against PPARγ, NAD-dependent deacetylase sirtuin-3 (SIRT3), cytochrome c (CYTO C), LKB1, pLKB1 (Ser428), ACC, pACC (Ser79), AMPKα (Thr172) and pAMPKα were purchased from Cell Signaling Technology (Beverly, MA, USA); the antibody against cell death activator CIDE-A (CIDEA) was purchased from Abnove (Taipei, Taiwan); the antibody against PR domain containing 16 (PRDM16), hormone sensitive lipase (HSL) and adipose trigyceride lipase (ATGL) were purchased from Abcam Inc. (Cambridge, MA, USA), and the antibodies

against C/EBPα, UCP1, PGC1α and glyceraldehyde-3-phosphate dehydrogenase (GAPDH) were purchased from Santa Cruz Biotechnology.

11. AMPK gene silencing by small interfering RNA (siRNA)

Predesigned siRNA against AMPK and negative control siRNA were purchased from Invitrogen (Carlsbad, CA, USA). Transfection into 3T3-L1 cells was performed with Lipofectamine RNAiMAX (Invitrogen) according to the manufacturer's instructions.

12. TC, TG and Ketone body measurement

TC and TG levels in HepG2 cell lysates were measured using a HDL and LDL/VLDL Cholesterol Assay Kit (ab65390, Abcam) and Triglyceride Quatification Assay Kit (ab65336, Abcam), respectively. Ketone bodies release in the HepG2 culture medium was measured using the Ketone Body Assay Kit (MAK134, Sigma-Aldrich).

13. Mitochondrial microscopic analysis

Mitochondrial analysis was performed as previously described (25).

14. Immunofluorescence (IF) assay

For IF assays, the cells were fixed with 4% paraformaldehyde in PBS for 15 min. and permeabilized with 0.2% Triton X-100 (Sigma) for 10 min., and thereafter, unspecific binding sites were blocked using PBS with 1% BSA (Calbiochem, La Jolla, CA, USA). Alexa 594 (1:500, Invitrogen) was used as a secondary antibody for UCP1 primary antibody (1:200). Alexa 488 (1:500, Invitrogen) was used as a secondary antibody for PGC1α (1:500), HSL (1:50) and HSL (1:500) primary antibodies. Fluorescence signals were imaged with a Zeiss LSM 5 Pascal laser confocal microscope (Carl Zeiss, Inc., Jena, Germany).

15. Immunohistochemical analysis

Immunohistochemistry analysis was performed as previously described (31). Antibodys for translocase of the outer membrane subunit 20 (TOM20) and UCP1/2/3 were purchased from Santa Cruz Biotechonology.

16. Temperature measurements

Temperature analysis was performed using an infrared camera (E60: Compact-Infrared-Thermal-Imaging-Camera; FLIR, West Malling, Kent, UK) as previously described (32).

17. Cold tolerance test

A cold tolerance test was performed in 10-week-old mice. The animals were exposed to a cold room (4 ℃) for 6 h without food or water. The rectal temperature was measured at the indicated time after exposure to the cold.

18. Statistical analysis

Data are expressed as the mean ± standard deviation (s.d.) of independent experiments. Significant differences between groups were determined with the Kruskal–Wallis test. All statistical analyzes were done with SPSS statistical analysis software version 11.5 (SPSS Inc., Chicago, IL, USA).

III. RESULTS

1. VA decreases weight gain and suppresses adipogenic factors in HFD-induced obese C57BL/6J mice

To investigate the anti-obesity effects of VA, we conducted an *in vivo* experiment with C57BL/6J mice. After inducing obesity by feeding HFD for 4 weeks, the mice were into five groups: a HFD induced mice group, a HFD group fed with 10, 100 and 1,000 mg/kg/day of VA, and a HFD group with EGCG. All groups had similar body weights at the beginning of the study. There were no significant differences in food intake between groups. (Data not shown). However, the mice fed with HFD diet gained significantly more weight than those fed with normal chow diet (ND) ($p < 0.05$). On the other hand, weight gain from VA was significantly less than that from the HFD. At the end point of the experiment, the average weight of the HFD group was 42.56 ± 1.83 g, while the average weight of mice fed with 10, 100, and 1,000 mg/kg/day VA and EGCG groups were 38.68 ± 3.18 g, 37.33 ± 1.87 g, 38.20 ± 1.64 g and 37.15 ± 2.70 g, respectively (Fig. 1A). The HFD-fed mice showed a significant increase in adiposity measured by the amount of WAT compared to the ND-fed mice ($p < 0.05$). The significance reduction of weight in WAT was determined in 10 and 100 mg/kg/day VA-fed mice. However, 1,000 mg/kg/day VA- and EGCG-fed mice certainly showed a relatively reduced body weight compared to the HFD-fed mice, but both did not show any significant difference in WAT weight. Liver weights of the VA- and EGCG-treated mice were nearly as low as that of the ND mice and differed significantly from the liver weights of the HFD-fed groups ($p < 0.05$) (Fig. 1B). There were no significant differences in body temperature between all groups (Fig. 1C). A serum parameter analysis was done to measure the serum LDL, HDL, TC and TG levels. VA significantly attenuated the levels of LDL and TC in the HFD-fed mice ($p < 0.05$), which indicates improvement in obesity (Fig. 1D). FFA levels in the serum was also measured. Mice fed with 100 and 1,000 mg/kg/day of VA showed reduced levels of FFA (Fig. 1E). Then, an H&E assay was performed to evaluate fat accumulation in tissues (Fig. 2A). Histopathology of the liver tissues (upper panels) and WAT (lower panels) showed that the lipid contents of the VA group were lower than those of the HFD control group. In the WAT and liver, the size of the adipocytes in the VA group was smaller than that of the HFD-fed group (Fig. 2A). Additionally, VA and EGCG treatment suppressed two key adipogenic factors, PPARγ and C/EBPα in WAT and liver tissues. The levels of pLKB1 and pAMPKα were also

increased in the VA group while the level of total LKB1 and the AMPKα levels were unchanged, indicating activated LKB1 and AMPKα by VA treatment (Fig. 2B and C).

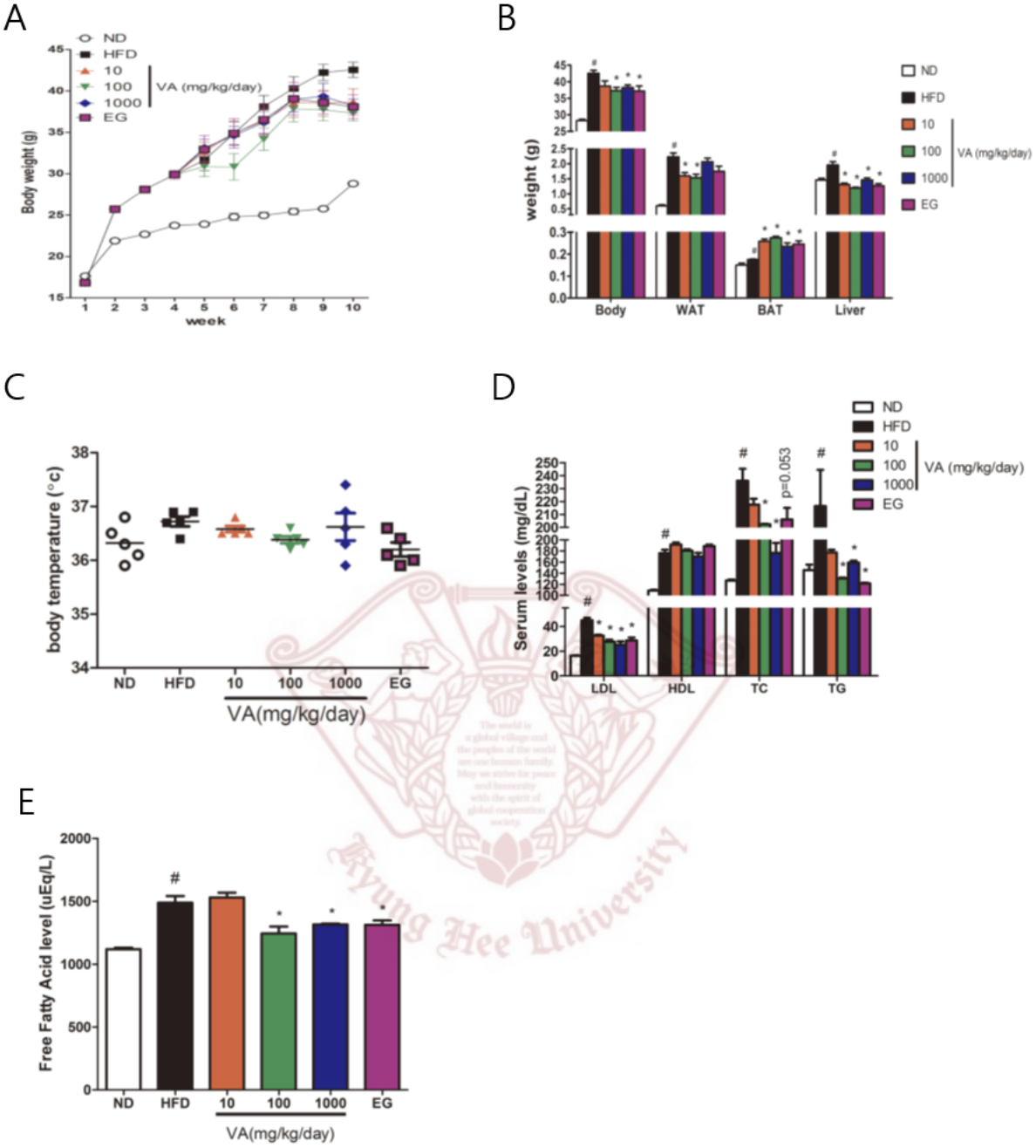

Figure 1. Effects of VA on obesity-related parameters in HFD-induced obese mice.

Mice were administered VA (10, 100 and 1,000 mg·kg^{-1} per day) with a HFD for 6 weeks. EGCG (20 mg·kg^{-1} per day) was administered as a positive control. (A) Changes in body weight were measured (ND, white circle; HFD, black square; VA 10 mg·kg^{-1} per day, red triangle; VA 100 mg·kg^{-1} per day, green inverted triangle; VA 1,000 mg·kg^{-1} per day, green blue diamond; EGCG, purple square). (B) The weights of the body, WAT, BAT and liver tissues of the mice were evaluated. (C) Core body temperature of each group was measured. (D-E) Serum LDL-cholesterol, HDL-cholesterol, total cholesterol (TC), triglyceride (TG) and

free fatty acid (FFA) levels were evaluated. The data are expressed as the mean ± s.d. and were analyzed with the Kruskal–Wallis test. $^{\#}p < 0.05$ significantly different from the ND group; $^{*}p < 0.05$ significantly different from the HFD group. EG, EGCG.

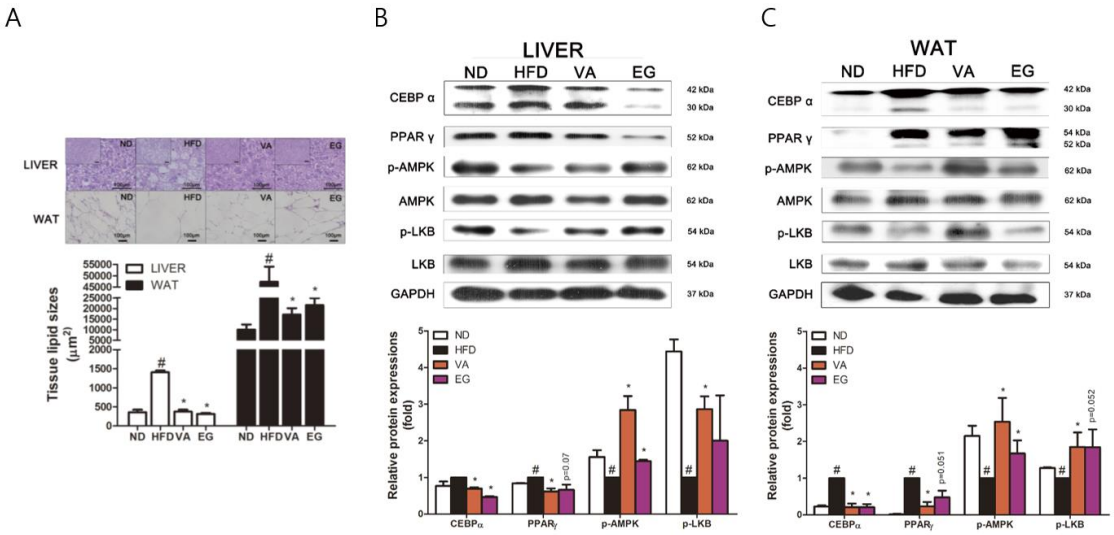

Figure 2. Effects of VA on changes in liver and white adipose tissue of HFD-induced obese mice.

(A) Paraffin sections of livers (upper panels) and WAT (lower panels) from ND mice, HFD mice, VA mice and EGCG mice were stained with H&E, and the histological changes were observed (magnification ×200, scale bar = 100 μm). (B-C) C/EBPα, PPARγ, pAMPK and pLKB1 protein levels were analyzed in the WAT and liver tissues by Western blot analysis. Densitometric analyses are presented as the relative ratios of GAPDH. The data are expressed as the mean ± s.d. and were analyzed with the Kruskal–Wallis test. $^{\#}p < 0.05$ significantly different from the ND group; $^{*}p < 0.05$ significantly different from the HFD group. EG, EGCG.

2. VA activates AMPK in liver and WAT of *db/db* mice

After a four-week-experiment using genetically engineered obese *db/db* mice, the *db/db* group gained significantly more weight than that of the WT group ($p < 0.05$). The *db/db* group had a body weight of 49.12 ± 0.15 g, which was higher by 21.55 g compared to the WT group (27.57 ± 0.53 g). However, the VA treated group (46.26 ± 0.11 g) showed a decrease by 2.85 g when compared to *db/db* group (Fig. 3A). Fig. 3B shows the effect of VA on the inguinal WAT (iWAT), epididymal WAT (eWAT), BAT and liver tissue weight in mice. VA significantly reduced the weights of both WATs and the liver in the mice. On the other hand, BAT was increased by VA ($p < 0.05$). The *db/db* mice had an increased food intake compared to the WT group, while no significant differences in food intake were observed between the *db/db* and *db/db* + VA groups (Fig. 3C). Next, a serum parameter analysis was done. Among the levels of TG, GLUCO, TC, HDL and LDL, VA significantly attenuated the levels of GLUCO in the *db/db* group, while HDL was increased by VA ($p < 0.05$) (Fig. 3D). Histological assays on the liver tissues showed that the lipid contents in the VA group were lower than those in the *db/db* group. The color of liver tissue was also restored similarly to the WT group (Fig. 4A). To confirm the effects of VA on adipogenesis in the *db/db* mice, we performed further assays using the adipose tissues of mice. VA reduced protein levels of C/EBPα and PPARγ in the liver, eWAT, and iWAT tissues. The phosphorylation levels of LBK1 and AMPK were also increased, consistent with results from HFD-fed mice (Fig. 4B and C). These results suggest that VA is able to attenuate adipogenesis in adipose tissue and also decrease steatosis in the liver.

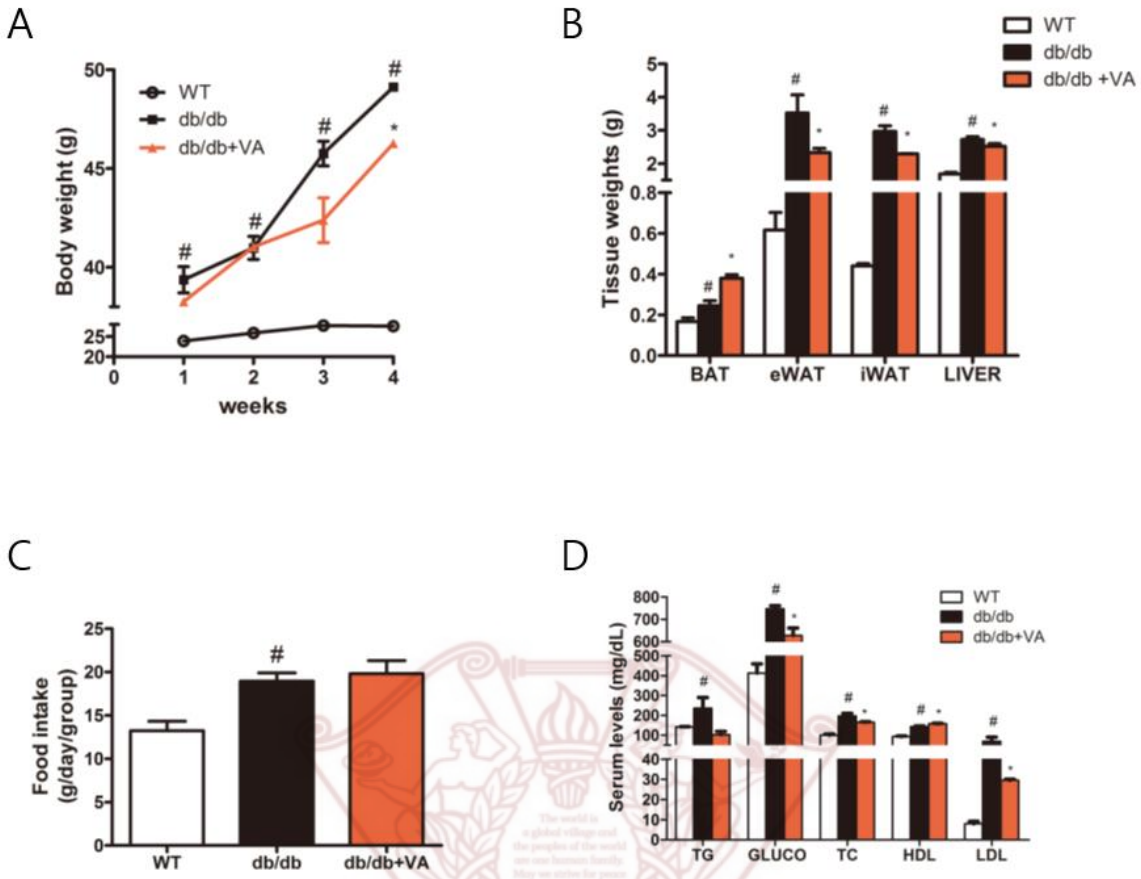

Figure 3. Effects of VA on obesity-related parameters in genetically obese *db/db* mice. Mice were administered VA (100 mg·kg-1 per day) for 4 weeks. (A) Changes in body weight were measured (WT, grey circle; *db/db*, black square; *db/db* with VA, grey triangle). (B) The weights of the eWAT, iWAT, liver and BAT of the mice were measured. (C) Food intake of each group was measured. (D) Serum TG, GLUCO, TC, HDL and LDL were evaluated. The data are expressed as the mean ± s.d. and were analyzed with the Kruskal–Wallis test. $^{\#}p < 0.05$ significantly different from WT group; $^{*}p < 0.05$ significantly different from *db/db* group.

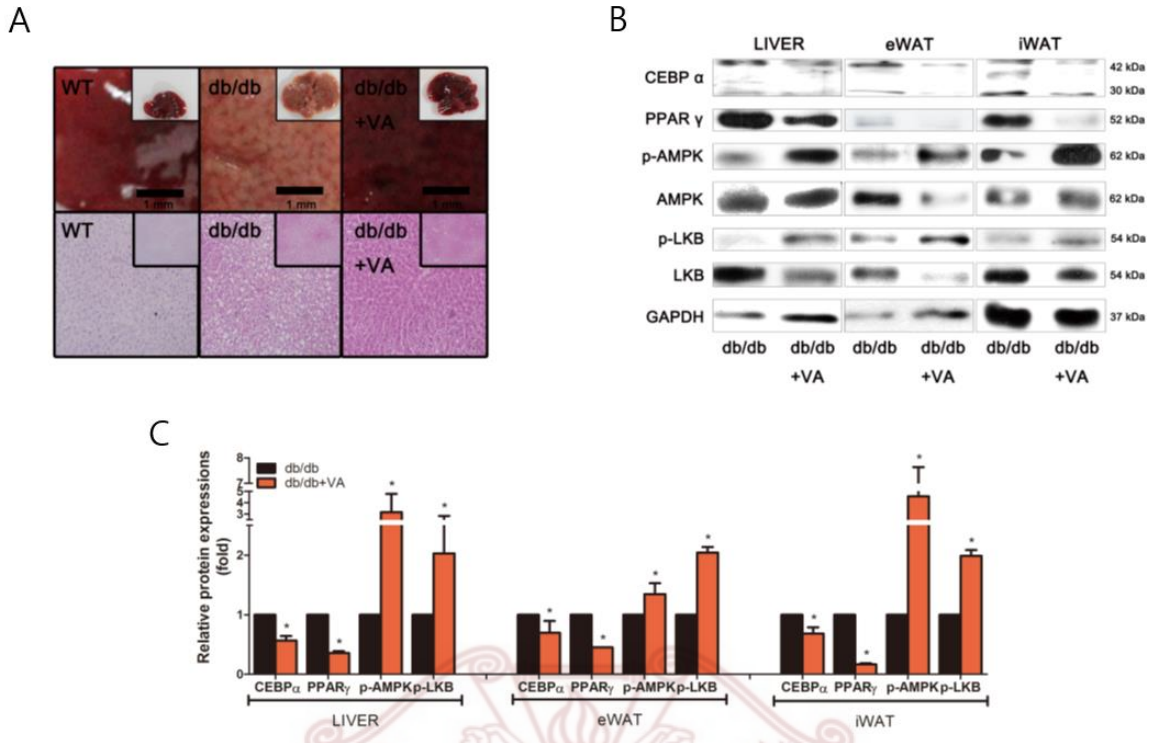

Figure 4. Effects of VA on changes in liver and white adipose tissue of genetically obese *db/db* mice.

(A) Paraffin sections of the livers (upper panels) and WAT (lower panels) from WT mice, *db/db* mice, and *db/db* mice treated with VA (100 mg·kg^{-1}) were stained with H&E, and the histological changes were observed (magnification ×200, scale bar = 100 μm). (B-C) Effects of VA on the C/EBPα, PPARγ, pAMPK and pLKB1 protein levels were analyzed in the liver tissues, eWAT and iWAT by Western blot analyses. Densitometric analyses are presented as the relative ratios of GAPDH. The data are expressed as the mean ± s.d. and were analyzed with the Kruskal–Wallis test. $^{\#}p < 0.05$ significantly different from WT group; $^{*}p < 0.05$ significantly different from *db/db* group.

3. VA attenuates liver steatosis by increasing mitochondrial activity in the liver

To confirm the effects of VA in the lever, we evaluated parameters related in liver biology, including hepatotoxicity and lipid metabolism. At the given doses, long-term treatment of VA did not seem to induce hepatic toxicity, as by the plasma activities of AST and ALT, the well-known enzyme parameters of liver injury (33) were within ranges similar to those of the normal control group (Fig. 5A). However, VA treatment did not show any significant changes in AST and ALT in *db/db* mice (Data not shown). We also observed reduced TG, TC and LDL levels in the liver tissues of both HFD-induced obese mice and *db/db* mice fed with VA (Fig. 5B). We then performed western blot assays on inflammatory markers, which are tightly related in liver toxicity and fat accumulation (34-36). VA decreased protein levels of NF-κB and COX-2 in the liver of HFD-fed and *db/db* mice (Fig. 5C). Next, we investigated FA oxidation, FA synthesis and mitochondrial activity in the liver. Real-time RT-PCR results showed increased gene levels of critical factors for biogenesis and oxidative phosphorylation of mitochondria including *Atp5a1*, *Nrf1* and *Nrf2*. It also enhanced *Atgl, Hsl, Acadm, Cpt1a* and *Ppargc1b*, factors associated with FA oxidation. VA treatment decreased factors indicating FA synthesis such as *Srebp1c* and *Fasn* were decreased in HFD-obese mice (Fig. 5D).

In addition, we also performed *in vitro* studies using the hepatocyte cell line HepG2. To investigate the cytotoxicity of VA, HepG2 cells were treated with various concentrations of VA (0-20 μM) and MTS analysis was performed for determining cytotoxicity (Data not shown). To determine the effect of VA on lipid accumulation in HepG2 cells, an Oil red-O staining was performed. After inducing lipid accumulation in HepG2 cells, VA (0-10 μM) was treated for 24 h. Among the concentrations, 10 μM of VA showed decrease of lipid accumulation ($p < 0.05$), suggesting that high concentration of VA suppresses adipogenesis in HepG2 cells (Data not shown). Further assays evaluating TG and TC levels confirmed that VA reduced TG and TC contents in HepG2 cells as well as lipid accumulation (Fig. 6A). To confirm the effects of VA on adipogenesis and inflammation in HepG2 cells, we performed western blot assays. As results, VA suppressed the protein expression levels of two inflammatory markers, NF-κB and COX-2, and two adipogenic markers, C/EBPα and PPARγ. Furthermore, the pAMPKα were also increased by VA treatment (Fig. 6B). Then, to evaluate the effect of VA on FA oxidation, we analyzed the concentration of ketone bodies. VA at 10 μM increased ketone body levels in the culture media when compared to untreated HepG2 cells, indicating increased FA oxidation by VA treatment (Fig. 6C). We also assessed the expression of HSL and ATGL, two lipases

closely related in FA oxidation. Consequent to the vivo results on Hsl and Atgl genes, VA treatment (10 μM) significantly up-regulated levels of HSL and ATGL when confirmed by western blot analyses (Fig. 6D) and IF staining (Fig. 6E). Next, FFA-induced HepG2 cells were stained with Mito-Tracker Red to determine whether VA affects mitochondrial activity. As shown in Fig. 6F, VA increased the number and activity of mitochondria.

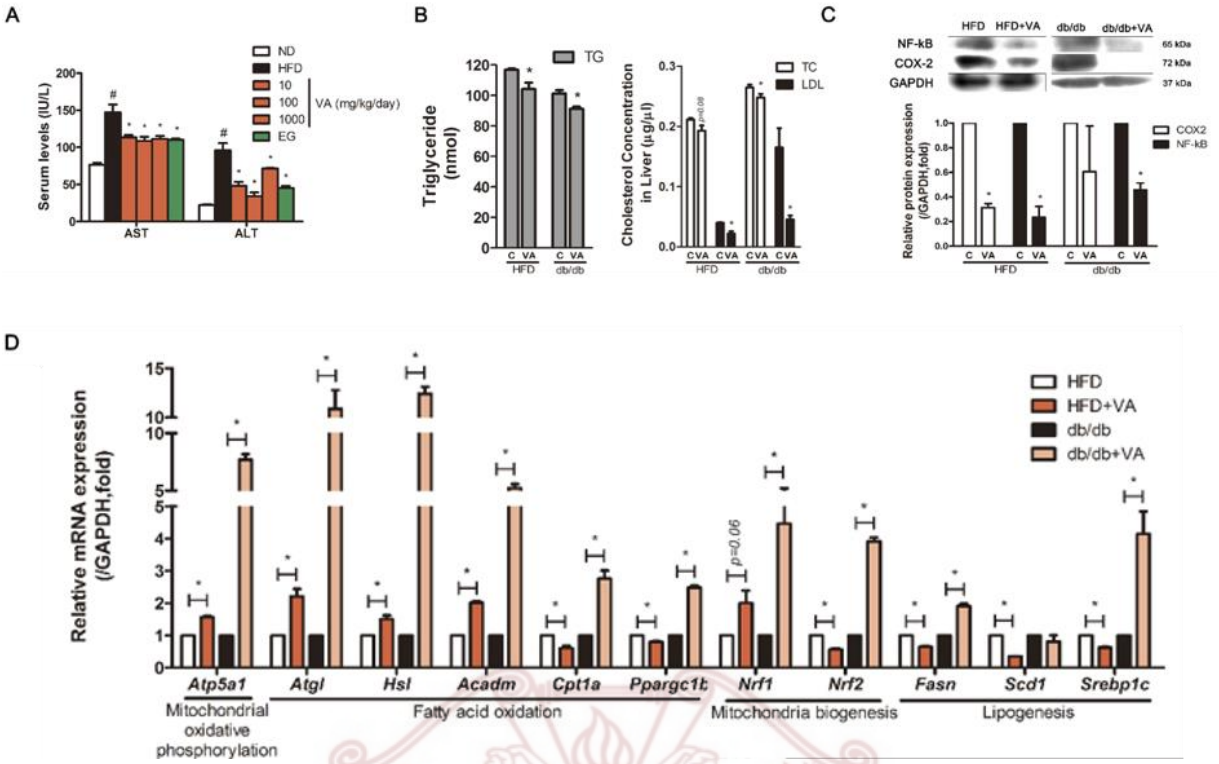

Figure 5. Effects of VA on liver metabolism in HFD-induced obese mice.

(A) Serum AST and ALT was evaluated in HFD mice. (B) Liver triglyceride, total cholesterol and LDL-cholesterol were evaluated. (C) Inflammatory factors COX-2 and NF-κB protein expressions were analyzed in the liver tissues of *db/db* and HFD mice by a Western blot analysis. (D) The mRNA levels of genes related in mitochondrial oxidative phosphorylation (*Atp5a1*), fatty acid oxidation (*Atgl, Hsl, Acadm, Cpt1a* and *Ppargc1b*), mitochondrial biogenesis (*Nrf1* and *Nrf2*) and lipogenesis (*Fasn, Scd*1 and *Srenp1c*) were analyzed in the liver tissues of *db/db* and HFD mice by real-time RT-PCR. The relative mRNA level of each gene was normalized to the level of *Gapdh*. Data are expressed as the mean ± s.d. and were analyzed with the Kruskal–Wallis test. $^{\#}p < 0.05$ versus undifferentiated control cells; $^{*}p < 0.05$ versus differentiated control cells.

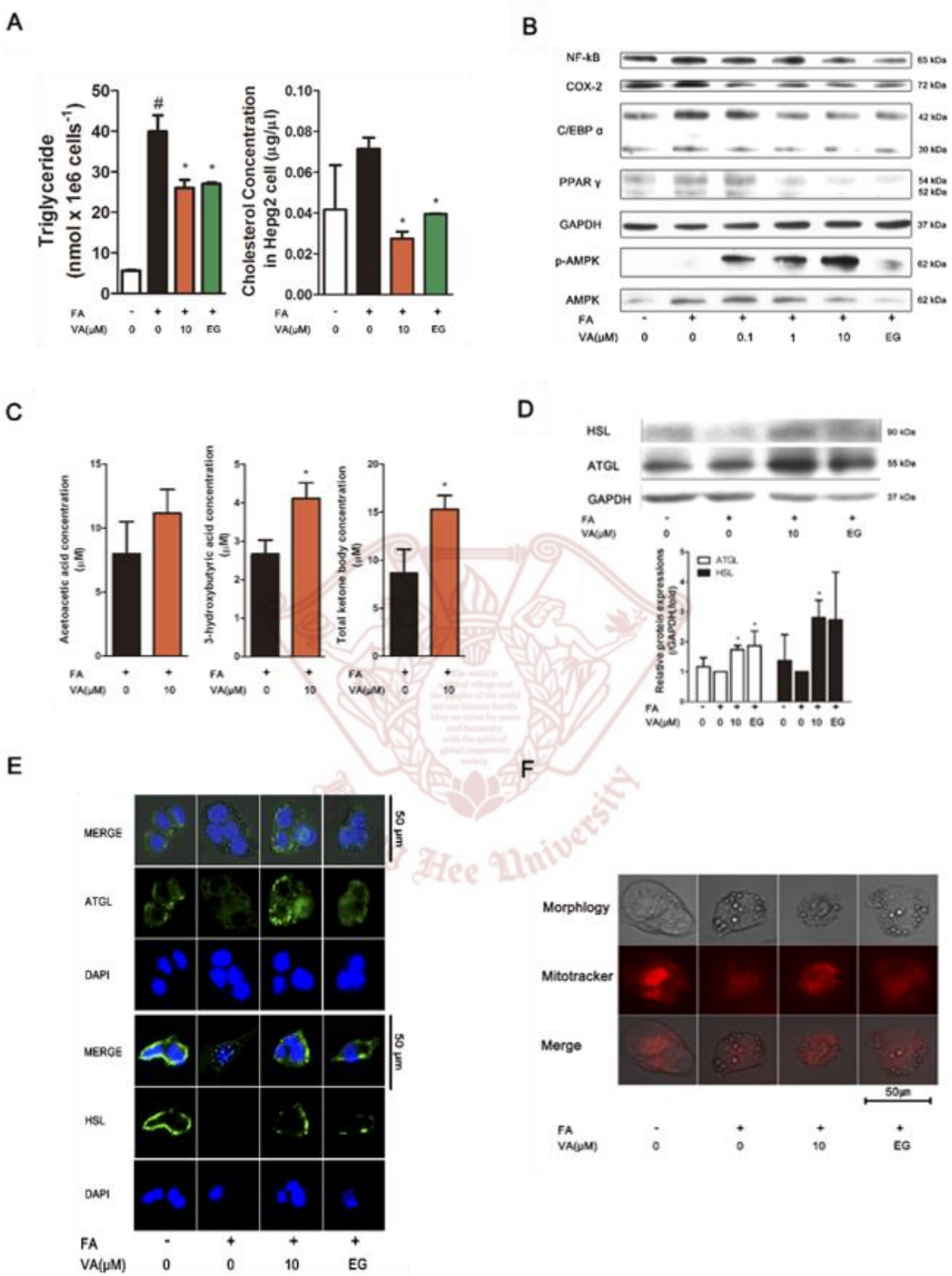

Figure 6. Effects of VA on liver metabolism in HepG2 cells.

(A) Triglyceride and total cholesterol in VA-treated HepG2 cells were measured. (B) Effects of VA on the NF-κB, COX-2, C/EBPα, PPARγ, and pAMPKα protein levels were analyzed in

HepG2 cells by Western blot analyses. (C) Ketone body concentration was measured in culture media of VA-treated HepG2 cells. (D-E) Expressions of FA oxidation markers ATGL and HSL were analyzed in the HepG2 cells by a Western blot analysis and immunofluorescence staining. (F) Mitochondrial abundance was analyzed in HepG2 cells by Mito-Tracker Red staining. Densitometric analyses are presented as the relative ratios of GAPDH. Data are expressed as the mean ± s.d. and were analyzed with the Kruskal–Wallis test. $^{\#}p < 0.05$ versus undifferentiated control cells; $^{*}p < 0.05$ versus differentiated control cells.

4. VA decreases lipid accumulation by suppressing adipogenic factors in white 3T3-L1 adipocytes

More experiments were carried out to investigate detail action mechanisms of VA. First, to determine the cytotoxicity of VA, an MTS assay was performed in VA (0–50 μM)-treated 3T3-L1 cells (Data not shown). Based on the results, all further experiments were done at concentrations of 0.1–10 μM.

Next, to investigate the effects of VA on preadipocyte differentiation, lipid accumulation was measured with the Oil Red-O staining assay after full differentiation with a 48-hour-exposure to 0, 0.1, 1, and 10 μM of VA. One and 10 μM of VA suppressed lipid accumulation in the 3T3-L1 adipocytes ($p < 0.05$) suggesting that VA inhibits adipogenesis in 3T3-L1 cells. EGCG (EG), GW9662 (GW) (37), and troglitazone (TRO) (38) were used as positive and negative controls, respectively (Fig. 7A and B). We also showed that VA treatment resulted in a dose-dependent suppression of C/EBPα and PPARγ at the protein level (Fig. 7C and D). Expressions of both adipogenic genes *Cebpa* and *Pparg* were also significantly decreased by VA confirmed by real-time RT-PCR analysis (Fig. 7E). In addition, we examined the effects of VA on the expression of the adipogenic genes *Lipin1*, *Retn*, *Fabp4* and *AdipoQ* in the 3T3-L1 cells, which resulted in a significant decrease of all adipogenic genes by the VA treatment (Fig. 7F).

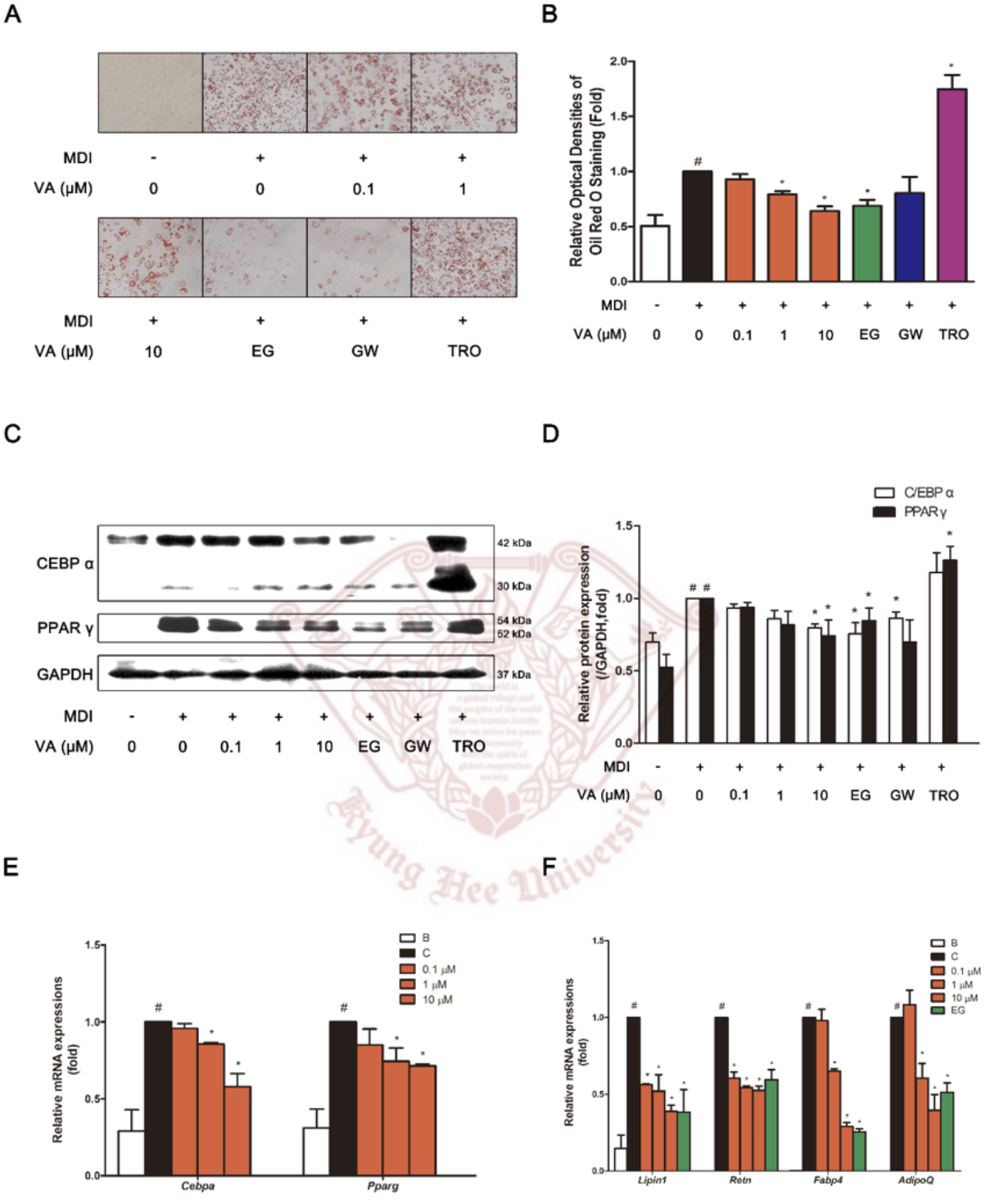

Figure 7. Effects of VA on adipocyte differentiation in 3T3-L1 cells.

(A) Post-confluent 3T3-L1 cells were differentiated in the absence or presence of VA (0, 0.1, 1, and 10 μM) for 6 days. Lipid droplets were measured by Oil Red-O staining. (B) The lipid content was quantified by measuring the absorbance. EGCG, GW, and TRO were used as

positive and negative controls. (C-D) Post-confluent 3T3-L1 cells were differentiated in the absence or presence of VA (0.1, 1, and 10 μM) for 6 days. C/EBPα and PPARγ protein expressions were analyzed by Western blot analysis. (E) The mRNA levels of *Pparg* and *Cebpa* were analyzed by real-time RT-PCR. (F) The mRNA levels of adipogenic and adipokine genes (*Fabp4*, *Retn*, *Lipin1*, and *AdipoQ*) were analyzed by real-time RT-PCR. The relative mRNA level of each gene was normalized to the level of *Gapdh*. Densitometric analyses are presented as the relative ratios of GAPDH. Data are expressed as the mean ± s.d. and were analyzed with the Kruskal–Wallis test. $^{\#}p < 0.05$ versus undifferentiated control cells; $^{*}p < 0.05$ versus differentiated control cells.

5. VA inhibits adipogenic factors through the AMPK pathway in white 3T3-L1 adipocytes

To investigate whether AMPK, a key player in energy homeostasis, was involved in the action of VA during 3T3-L1 differentiation, the protein levels of pAMPKα were analyzed. It has been reported that the AMPK pathway is regulated by EGCG during adipogenesis (24); therefore, EGCG was used as a positive control. As shown in Fig. 8A and B, cells treated with VA showed increased levels of pAMPKα in a dose-dependent manner while the total levels of AMPKα were unchanged. The tumor suppressor LKB1, an upstream kinase and also a regulator of AMPK, also showed induced phosphorylation levels by the treatment with VA. Furthermore, increased pACC, the downstream target of AMPKα, was observed from the VA treatment (Fig. 8A and B).

To confirm the above results, adipocytes were pre-treated with AMPKα siRNA and then treated with 10 μM of VA. As shown in Fig. 8C, AMPKα protein levels were reduced by AMPKα siRNA transfection. When AMPKα was blocked by siAMPKα, VA failed to decrease the expressions of C/EBPα and PPARγ, which were significantly inhibited in the siControl + VA group (Fig. 8D and E). This suggests that the action of VA was dependent on the AMPK pathway.

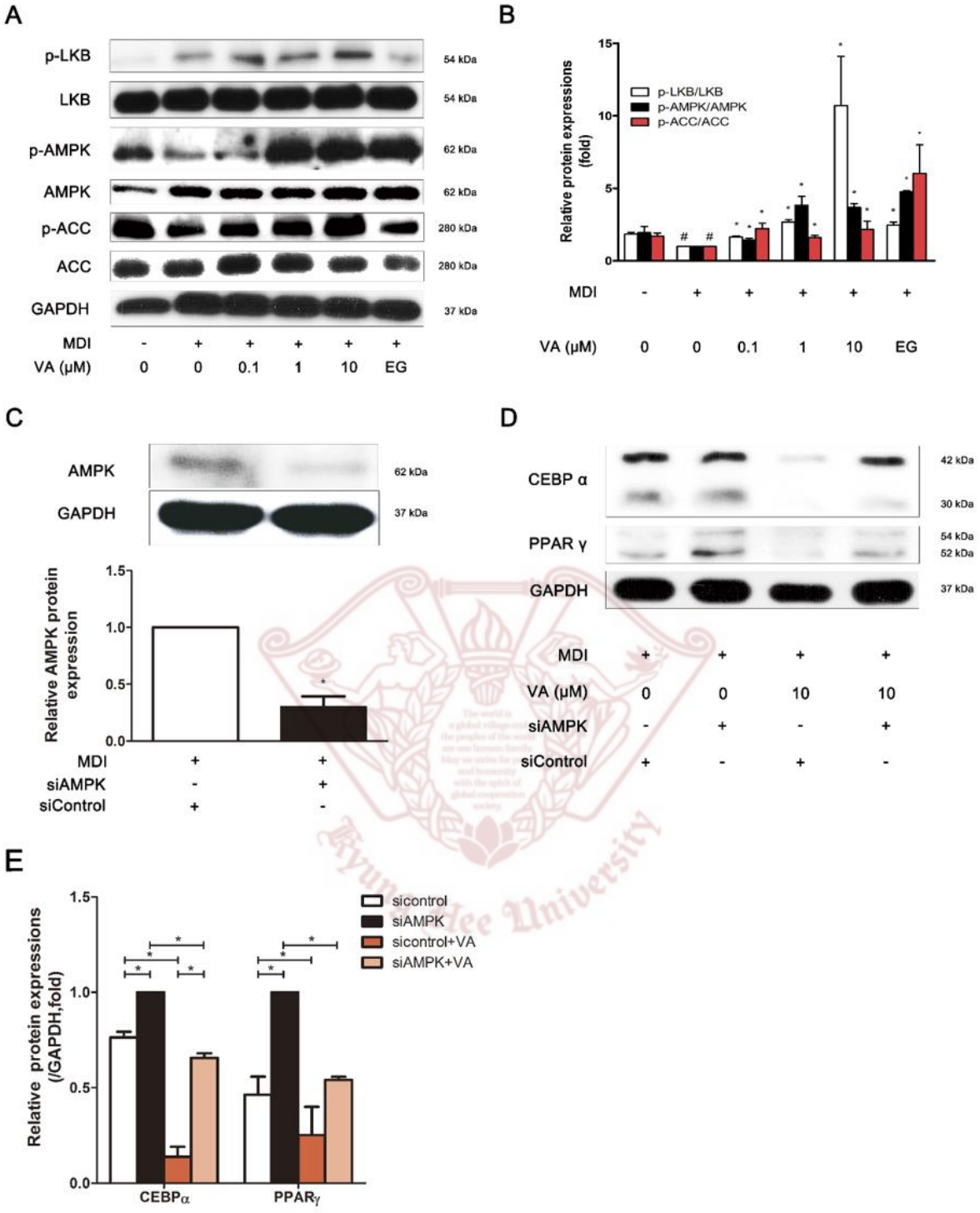

Figure 8. Effects of VA on activation of AMPK signaling in 3T3-L1 cells.

(A-B) Post-confluent 3T3-L1 cells were differentiated in the absence or presence of VA (0.1,1 and 10 μM) for 6 days. pLKB1, pAMPKα, and pACC protein levels were determined by Western blot analysis. GAPDH was used as an internal control. EGCG was used as a positive control. (C) Expression of AMPKα was determined after treatment with siAMPKα (10 pM). (D-E) After AMPKα siRNA pretreatment and VA (10 μM) treated differentiation, the protein

expressions of C/EBPα and PPARγ were determined by Western blot analysis. Densitometric analyses are presented as the relative ratios of GAPDH. The data shown are representative of three independent experiments performed in triplicate. Data are expressed as the mean ± s.d. and were analyzed with the Kruskal–Wallis test. $^{\#}p < 0.05$ versus undifferentiated control cells; $^{*}p < 0.05$ versus differentiated control cells.

6. VA activates thermogenesis-related genes in BAT and primary cultured brown adipocytes

The role of AMPK in BAT activation is well known due to the close relationship between AMPKα and PGC1α. Because the effect of VA on AMPK activation was verified, we expected VA to be a BAT-activating agent as well. Therefore, we investigated BAT activating features of VA by performing assays to evaluate changes in thermogenesis-related factors in the BAT of both *db/db* and HFD mice. Western blot analyses show that VA treatment resulted in increased PGC1α and UCP1 in BAT (Fig. 9A).

We then investigated the effect of VA on FA oxidation and mitochondrial oxidative phosphorylation. Real-time RT-PCR results showed significant increase in gene levels of factors for mitochondrial oxidative phosphorylation and FA oxidation such as *Atp5a1, Atgl, Hsl, Acadm, Cpt1a* and *Ppargc1b* (Fig. 9B). VA-treated mice showed increased skin temperature at the interscapular BAT region when compared with HFD (Fig. 9C). The mitochondrial preprotein TOM20 is a multisubunit protein complex that facilitates the import of nucleus-encoded precursor proteins across the mitochondrial outer membrane (39). Therefore, we measured the expression of TOM20 to estimate the amount of mitochondria, and the expression of UCP1/2/3 in order to evaluate the effect of VA on thermogenesis. The immunostaining of BAT showed elevated levels of TOM20 and UCP1/2/3 in the VA-fed mice (Fig. 9D).

We further evaluated the effect of VA on thermogenesis in mice by performing a cold stress test. After a 6-h-cold-stimulation, body core temperature of ND-fed mice dropped down to 31.26 ± 0.45 ℃, which took 20 min to recover back to the normal body temperature (36-37 ℃). In the VA treatment group, core body temperature was significantly higher than that of HFD (35.12 ± 0.64 ℃ vs. 33.93 ± 0.67 ℃), which was also rapidly restored to normal temperature level within 20 min. On the other hand, HFD-fed control mice failed to restore their body temperature after 20 min acclimation at RT, suggesting the thermogenic action was due to VA administration (Fig. 9E). Therefore, our hypothesis on the role of VA in BAT activation was shown *in vivo*.

To confirm the BAT-activating effect of VA, we performed *in vitro* studies using primary cultured brown adipocytes. To determine the cytotoxicity of VA in primary brown adipocytes, the cells were treated with various concentrations (0–10 μM) of VA, and an MTS assay was performed. Treatment with 0.1 and 1 μM of VA did not cause any cytotoxicity in brown adipocytes (Data not shown). Next, to investigate the effects of VA on brown adipocyte

differentiation, lipid accumulation was measured by Oil Red-O staining. VA (0.1 and 1 μM) significantly increased lipid accumulation in brown adipocytes (Fig. 10A). Real-time RT-PCR showed significantly enhanced levels of critical genes for thermogenesis and mitochondrial biogenesis including *Ucp1, Ppargc1a, Sirt3, Cyc* and *Lipin1* (Fig. 10B). We then confirmed the increase in related proteins. The levels of SIRT3, PGC1α, PRDM16, UCP1, CYTO C and CIDEA in primary brown adipocytes were significantly up-regulated by VA (Fig. 10C and D). We also performed IF analyses of PGC1α and UCP1, the specific markers of thermogenesis in brown adipocytes. As seen in Fig. 10E, PGC1α and UCP1 were expressed in differentiated brown adipocytes located in the cytoplasm which expression became higher by VA treatment compared to the non-treated cells.

One of the most crucial differences between white and brown adipocyte cells is the high number and activity of mitochondria located in brown adipocyte cells. To examine whether VA affects mitochondrial activity, differentiated brown adipocytes were stained with Mito-Tracker Red. The results show that VA increased the number and activity of mitochondria (Fig. 10F). Taken together, these results suggest that VA treatment increases energy expenditure by mediating the thermogenesis-related gene and protein expressions in BAT.

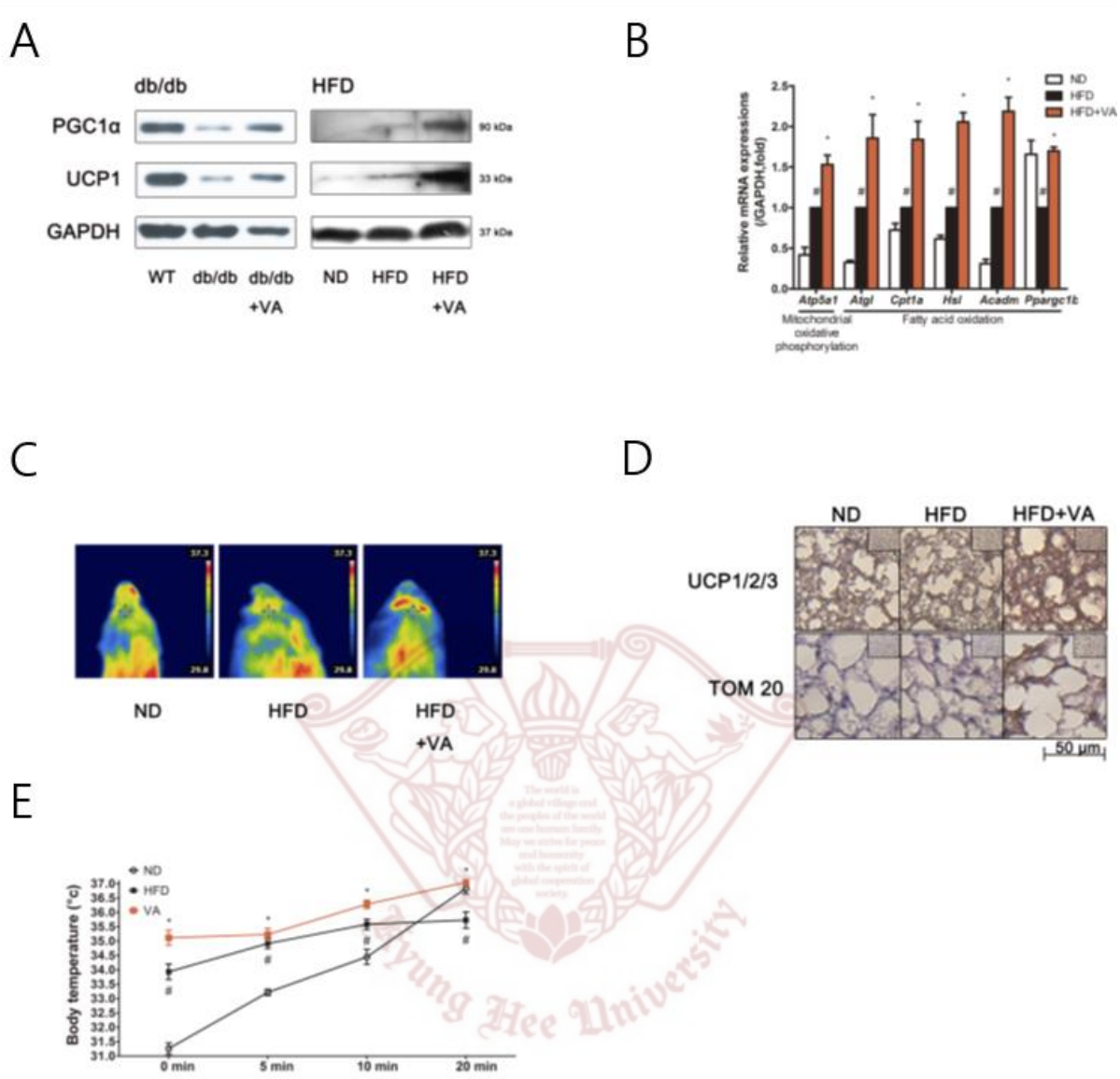

Figure 9. Effects of VA on thermogenic factors in brown adipose tissue of HFD-induced obese mice and genetically obese *db/db* mice.

(A) PGC1α and UCP1 protein levels were analyzed in the BAT of *db/db* and HFD mice by Western blot analyses. (B) The mRNA levels of genes related in mitochondrial oxidative phosphorylation (*Atp5a1)* and fatty acid oxidation (*Atgl, Hsl, Acadm, Cpt1a* and *Ppargc1b*) were analyzed in BAT of HFD mice by real-time RT-PCR. The relative mRNA level of each gene was normalized to the level of *Gapdh*. (C) Representative infrared thermal image. (D) Expressions of UCP1/2/3 and TOM20 were evaluated by an immunohistochemistry analysis. (E) Core body temperature of ND, HFD and VA-treated mice during cold challenge after being housed at 4℃. The relative mRNA level of each gene was normalized to the level of Gapdh.

Densitometric analyses are presented as the relative ratios of GAPDH. The data shown are representative of three independent experiments performed in triplicate. Data are expressed as the mean ± s.d. and were analyzed with the Kruskal–Wallis test. $^{\#}p < 0.05$ versus undifferentiated control cells, $^{*}p < 0.05$ versus differentiated control cells.

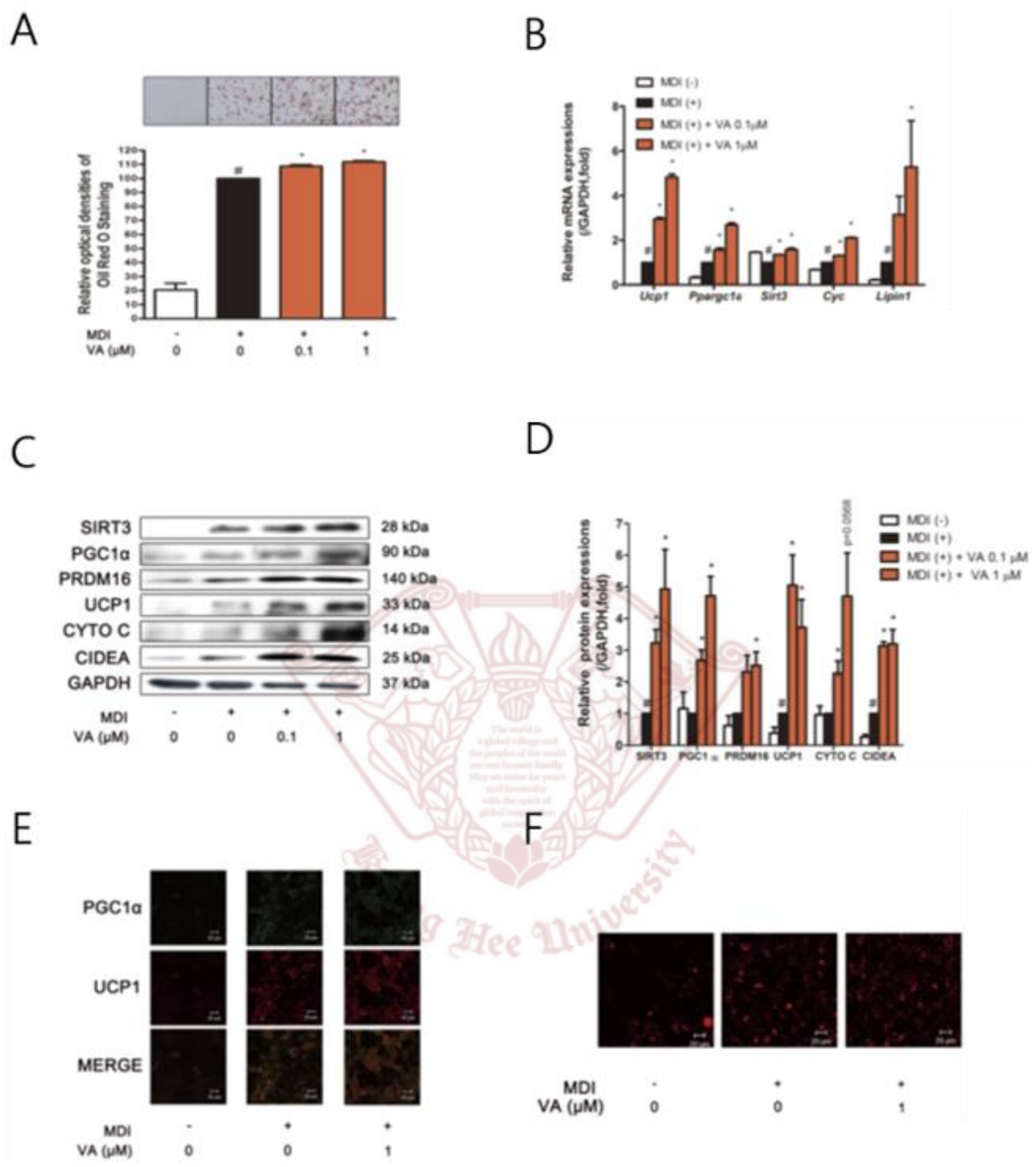

Figure 10. Effects of VA on thermogenic factors in primary cultured brown adipocytes.

(A) Lipid droplets were measured by Oil Red-O staining after the brown adipocyte cells were differentiated in the absence or presence of VA (0.1, and 1 μM). (B) At day 6 after induction, total RNA was isolated and the expressions of brown adipocyte markers *(Ucp1, Ppargc1a, Sirt3, Lipin1* and *Cyc*) were determined by real-time RT-PCR. (C-D) Protein extracts were prepared from the cultures at day 6, and the expression levels of brown adipocyte markers (UCP1, PGC1α, SIRT3, LIPIN1 and CYTO C) were determined by Western blot analyses. (E) Expressions of PGC1α and UCP1 were evaluated by immunofluorescence analysis. (F)

Mitochondrial abundance was analyzed by Mito-Tracker Red staining. The relative mRNA level of each gene was normalized to the level of *Gapdh*. Densitometric analyses are presented as the relative ratios of GAPDH. The data shown are representative of three independent experiments performed in triplicate. Data are expressed as the mean ± s.d. and were analyzed with the Kruskal–Wallis test. $^{\#}p < 0.05$ versus undifferentiated control cells, $^{*}p < 0.05$ versus differentiated control cells.

IV. DISCUSSION

Previous studies have provided much evidence on the availability of VA in regulating inflammatory or immune diseases. For instance, VA has hepatoprotective effects by suppressing immune-mediated liver inflammation (40). Another study suggested VA suppresses inflammation in ulcerative colitis (19). Because excessive obesity is associated with inflammation (41), these previous reports suggest that VA has a potential role in obesity control. Therefore, in this study, we investigated whether VA has any anti-obesity effects with *in vivo* and *in vitro* experiment models.

Fat tissue is a major organ involved in the development of obesity and consists of two types of adipose tissues in humans: WAT and BAT. They have opposite roles in maintaining energy homeostasis (42). Adipogenesis is a regulated cellular differentiation process, in which preadipocytes are transformed into mature adipocytes (43). During adipogenesis of 3T3-L1 cells, early-stage-expressed master regulators, C/EBPα and PPARγ, induce differentiation of ectopic expression in nonadipogenic fibroblasts (44, 45). PPARγ, a member of the nuclear receptor family, has been detected both in humans and mice. It acts as one of the key factors regulating glucose metabolism and involves in pathologies of various diseases such as obesity, cancer, and inflammation (46, 47). C/EBPα, a member of the basic region leucine zipper family of transcription factors, is involved in adipogenesis of the liver and adipose tissue. In the present study, VA treatment resulted in decreased expressions of PPARγ and C/EBPα in 3T3-L1 cells. Similarly, *in vivo* results showed that such factors were decreased by VA in WATs of *db/db* and HFD-fed mice. We also observed that VA treatment decreased the expressions of several adipokine and adipogenesis-related genes in 3T3-L1 adipocytes, including *Retn*, *Fabp4*, *AdipoQ* and *Lipin1*. Adipokines are water-soluble substances related to adipocytes (48), of which resistin, aP2 and adiponectin are all well-known representatives showing important roles in obesity (49, 50). These results support that VA inhibits adipogenesis by suppressing adipogenic factors.

Besides the adipose tissues, the liver is also an energy storing-organ involved in whole-body metabolism (51). It plays a central role in metabolic homeostasis by its role as the major site of synthesis and metabolism of carbohydrates, proteins and lipids (52, 53). The rapid increase in obesity worldwide is associated with the increase of lipid storage in the liver, leading to non-alcoholic fatty liver diseases (NAFLDs), especially in the western societies (54,

55). Our results show that VA attenuates hepatotoxicity/hepatitis while reducing fat accumulation and activating FA oxidation *in vivo* and *in vitro*, suggesting its possible use for NAFLD-related obesity.

AMPK is a major regulator of body energy homeostasis because it regulates hormones such as leptin and adiponectin, which are substances related to appetite and metabolism (49). AMPK is activated under situations of ATP exhaustion such as metabolic stress or exercise and regulates the AMP/ATP ratio by suppressing fatty acid and glucose consumption which leads to ATP production. AMPK activation includes AMP-mediated allosteric activation and phosphorylation of the threonine residue Thr172 located in the catalytic subunit of AMPK which is regulated by upstream kinases like LKB1 or CaMKIIβ (10, 11, 56-59). Activated AMPK causes phosphorylation and inactivation of ACC and 3-hydroxy-3-methylglutaryl-coenzyme A reductase which are all required for ATP consumption. AMPK also inhibits the expressions of genes related to lipid synthesis including fatty acid synthase, pyruvate kinase and ACC. The inactivated pACC results in a decreased level of malonyl-CoA and an increased activity of carnitine palmitoyltransferase-1 (CPT1) leading to increased FA oxidation in β-oxidation (12-14). In addition to ACC, AMPK has been shown to activate hormone-sensitive lipase (HSL) activity. When HSL is phosphorylated in response to protein kinase A (PKA) activating signals, it actively removes FAs from TG (60). Overexpression of AMPKα by AICAR or metformin in the liver of a normal group and obesity group increases the level of β-hydroxybutyrate, which is the growth indicator of lipid oxidation, and reduces blood TG. Besides its action on enzyme activities, activation of AMPK also affects the expression of a number of glycolytic/lipogenic enzymes in the liver and adipose tissue. Included in this list are the genes for fatty acid synthase (FAS), ACC and sterol regulatory element-binding proteins (SREBPs), key regulators of numerous lipogenic enzymes (61-63). This shows that AMPK mediates the balance of fat metabolism in the liver through reduced fat synthesis and lipolysis (64).

In our study, pAMPK and pLKB1 were increased in the liver tissues of both HFD-fed and *db/db* mice by VA. VA also suppressed fat accumulation in the liver tissue, and increased expressions of pAMPK and pLKB1 in the WAT of HFD-fed and *db/db* mice. Similarly, in adipocytes, VA treatment activated the AMPK pathway. We then pre-treated the adipocytes with siAMPKα to investigate the underlying mechanism of VA. The inhibition rates of PPARγ and C/EBPα, which were originally suppressed by VA treatment, were significantly reduced in

the siAMPKα-treated cells. This shows that the anti-adipogenic action of VA is due to activation of the AMPK signaling pathway, at least partially.

Based on several reports regarding the importance of AMPK in BAT activation, we then performed experiments on brown adipocyte-specific thermogenesis with the expectation that VA can induce it. Our results show that VA treatment in HFD-induced obese mice and genetically obese *db/db* mice resulted in increased UCP1 and PGC1α in BAT. Furthermore, mitochondria specific proteins as well as UCP1 and PGC1α in primary brown adipocytes were also increased by VA in a dose dependent manner. These results indicate that the anti-obesity effect of VA was due to the increased metabolic energy consumption through mitochondrial action. AMPK activation increases the expressions of mitochondria-related genes through PGC1α expression. By increasing cellular NAD^+ levels, AMPK activates the NAD-dependent deacetylase SIRT1, which results in deacetylation/activation of PGC1α (65-67). The reported relationship between AMPK and these brown adipocyte-related factors including PGC1α and mitochondria suggests that VA has thermogenic effects. BAT is responsible for consuming energy in the form of heat, which is a process called thermogenesis. In contrast to previous knowledge, recent studies have shown that BAT also exists in adult humans (68). Brown adipocytes, consisting of BAT, have a large quantity of mitochondria and specifically express a brown color. The inner membranes of mitochondria in these adipocytes possess the UCP1 protein (69). The thermogenic action of BAT is dependent on the activity of this particular protein, which responses to cold exposure (70, 71). Recent studies also identified that PGC1α is related to both the expression and action of UCP1 (72). Thermogenesis in BAT by UCP1 is an important part of energy consumption in rodents. According to a study by Baumruk *et al*., UCP1 overexpression in WAT led to reduced obesity by HFD (73). Therefore, UCP1 has gained recognition as a novel target in the field of obesity. We observed elevated skin temperature of the BAT region in VA-fed mice. After a 6 h-cold challenge test, VA-fed mice rapidly recovered its core body temperature to normal. Further analysis showing increase in mitochondrial and thermogenic factors by VA treatment suggests a possibility of VA as a thermogenic agent. However, further investigation is essential to confirm the detailed mechanism of VA on thermogenesis. Because the results of this study provide evidence for the AMPK-linked action of VA, the goal of our next study is to reveal the precise mechanisms of VA in brown adipocytes. Brief description of this study is summarized in Figure 11.

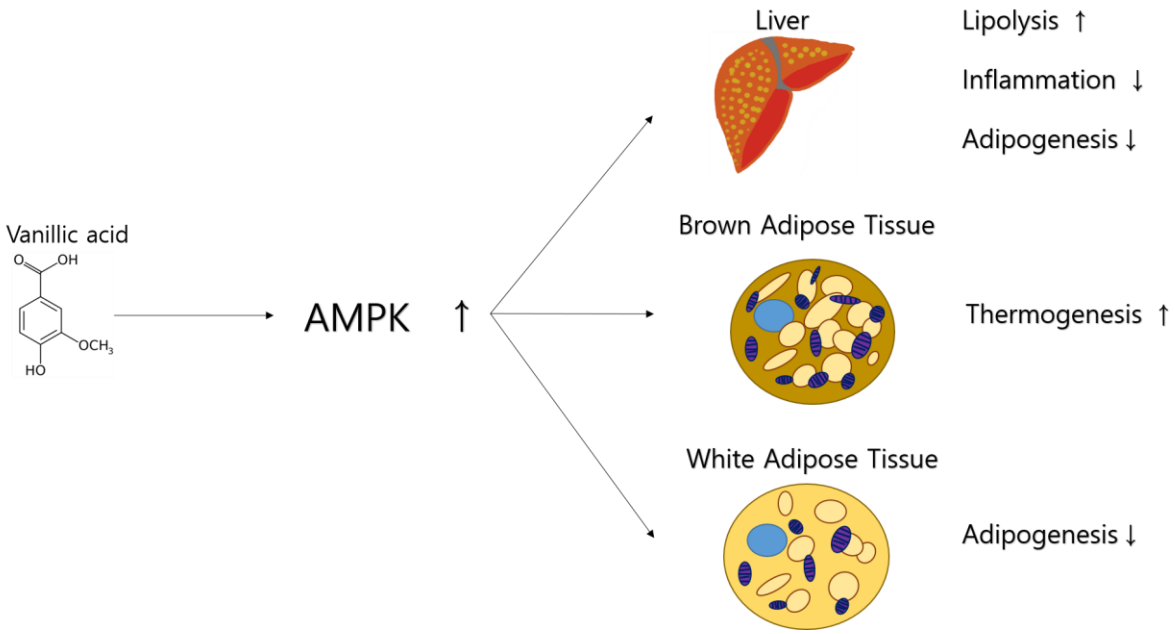

Figure 11. Diagrammatic visualization showing the contribution of VA to the pathological pathways of obesity.

V. CONCLUSIONS

In summary, our study shows the anti-obese action of VA *in vivo* and *in vitro*. VA significantly improved obesity in HFD-induced obese mice and *db/db* mice. In addition, VA treatment dramatically decreased the expressions of adipogenic markers in 3T3-L1 cells, which was due to AMPK activation. Furthermore, VA increased the expressions of mitochondrial and thermogenic factors in both BAT and primary cultured brown adipocytes. Taken together, VA possesses anti-obesity effects by increasing energy metabolism in white and brown adipocytes, suggesting its potential use in the field of obesity treatment.

VI. REFERENCES

1. Kopelman, P. G. (2000) Obesity as a medical problem. *Nature* **404**, 635-643
2. Stumvoll, M., Goldstein, B. J., and van Haeften, T. W. (2005) Type 2 diabetes: principles of pathogenesis and therapy. *Lancet* **365**, 1333-1346
3. Haslam, D. W., and James, W. P. (2005) Obesity. *Lancet* **366**, 1197-1209
4. Ogden, C. L., Carroll, M. D., Kit, B. K., and Flegal, K. M. (2014) Prevalence of childhood and adult obesity in the United States, 2011-2012. *JAMA* **311**, 806-814
5. Lee, H., Kang, R., Kim, Y. S., Chung, S. I., and Yoon, Y. (2010) Platycodin D inhibits adipogenesis of 3T3-L1 cells by modulating Kruppel-like factor 2 and peroxisome proliferator-activated receptor gamma. *Phytother. Res.* **24 Suppl 2**, S161-167
6. Lee, H., Bae, S., Kim, Y. S., and Yoon, Y. (2011) WNT/beta-catenin pathway mediates the anti-adipogenic effect of platycodin D, a natural compound found in Platycodon grandiflorum. *Life Sci.* **89**, 388-394
7. Kim, H. L., Park, J., Park, H., Jung, Y., Youn, D. H., Kang, J., Jeong, M. Y., and Um, J. Y. (2015) Platycodon grandiflorum A. De Candolle Ethanolic Extract Inhibits Adipogenic Regulators in 3T3-L1 Cells and Induces Mitochondrial Biogenesis in Primary Brown Preadipocytes. *J. Agric. Food Chem.* **63**, 7721-7730
8. Zhou, G., Myers, R., Li, Y., Chen, Y., Shen, X., Fenyk-Melody, J., Wu, M., Ventre, J., Doebber, T., Fujii, N., Musi, N., Hirshman, M. F., Goodyear, L. J., and Moller, D. E. (2001) Role of AMP-activated protein kinase in mechanism of metformin action. *J. Clin. Invest.* **108**, 1167-1174
9. Zhang, B. B., Zhou, G., and Li, C. (2009) AMPK: an emerging drug target for diabetes and the metabolic syndrome. *Cell Metab.* **9**, 407-416
10. Woods, A., Johnstone, S. R., Dickerson, K., Leiper, F. C., Fryer, L. G., Neumann, D., Schlattner, U., Wallimann, T., Carlson, M., and Carling, D. (2003) LKB1 is the upstream kinase in the AMP-activated protein kinase cascade. *Curr. Biol.* **13**, 2004-2008
11. Hawley, S. A., Pan, D. A., Mustard, K. J., Ross, L., Bain, J., Edelman, A. M., Frenguelli, B. G., and Hardie, D. G. (2005) Calmodulin-dependent protein kinase kinase-beta is an alternative upstream kinase for AMP-activated protein kinase. *Cell Metab.* **2**, 9-19

12. Foretz, M., Carling, D., Guichard, C., Ferre, P., and Foufelle, F. (1998) AMP-activated protein kinase inhibits the glucose-activated expression of fatty acid synthase gene in rat hepatocytes. *J. Biol. Chem.* **273**, 14767-14771
13. Woods, A., Azzout-Marniche, D., Foretz, M., Stein, S. C., Lemarchand, P., Ferre, P., Foufelle, F., and Carling, D. (2000) Characterization of the role of AMP-activated protein kinase in the regulation of glucose-activated gene expression using constitutively active and dominant negative forms of the kinase. *Mol. Cell Biol.* **20**, 6704-6711
14. Assifi, M. M., Suchankova, G., Constant, S., Prentki, M., Saha, A. K., and Ruderman, N. B. (2005) AMP-activated protein kinase and coordination of hepatic fatty acid metabolism of starved/carbohydrate-refed rats. *Am. J. Physiol. Endocrinol. Metab.* **289**, E794-800
15. Gomez-Lechon, M. J., Donato, M. T., Martinez-Romero, A., Jimenez, N., Castell, J. V., and O'Connor, J. E. (2007) A human hepatocellular in vitro model to investigate steatosis. *Chem. Biol. Interact.* **165**, 106-116
16. Chiu, H. C., Kovacs, A., Ford, D. A., Hsu, F. F., Garcia, R., Herrero, P., Saffitz, J. E., and Schaffer, J. E. (2001) A novel mouse model of lipotoxic cardiomyopathy. *J. Clin. Invest.* **107**, 813-822
17. Grishko, V., Rachek, L., Musiyenko, S., Ledoux, S. P., and Wilson, G. L. (2005) Involvement of mtDNA damage in free fatty acid-induced apoptosis. *Free Radic. Biol. Med.* **38**, 755-762
18. Sinha, A. K., Sharma, U. K., and Sharma, N. (2008) A comprehensive review on vanilla flavor: extraction, isolation and quantification of vanillin and others constituents. *Int. J. Food Sci. Nutr.* **59**, 299-326
19. Kim, S. J., Kim, M. C., Um, J. Y., and Hong, S. H. (2010) The beneficial effect of vanillic acid on ulcerative colitis. *Molecules* **15**, 7208-7217
20. Gálvez, M. C., Barroso, C. G., and Pérez-Bustamante, J. A. (1994) Analysis of polyphenolic compounds of different vinegar samples. *Z. Lebensm. Unters. Forsch.* **199**, 29-31
21. Calixto-Campos, C., Carvalho, T. T., Hohmann, M. S., Pinho-Ribeiro, F. A., Fattori, V., Manchope, M. F., Zarpelon, A. C., Baracat, M. M., Georgetti, S. R., Casagrande, R., and Verri, W. A., Jr. (2015) Vanillic Acid Inhibits Inflammatory Pain by Inhibiting

Neutrophil Recruitment, Oxidative Stress, Cytokine Production, and NFkappaB Activation in Mice. *J. Nat. Prod.* **78**, 1799-1808

22. Sindhu, G., Nishanthi, E., and Sharmila, R. (2015) Nephroprotective effect of vanillic acid against cisplatin induced nephrotoxicity in wistar rats: a biochemical and molecular study. *Environ. Toxicol. Pharmacol.* **39**, 392-404
23. Hsu, C. L., and Yen, G. C. (2007) Effects of flavonoids and phenolic acids on the inhibition of adipogenesis in 3T3-L1 adipocytes. *J. Agric. Food Chem.* **55**, 8404-8410
24. Hwang, J. T., Park, I. J., Shin, J. I., Lee, Y. K., Lee, S. K., Baik, H. W., Ha, J., and Park, O. J. (2005) Genistein, EGCG, and capsaicin inhibit adipocyte differentiation process via activating AMP-activated protein kinase. *Biochem. Biophys. Res. Commun.* **338**, 694-699
25. Jeong, M. Y., Kim, H. L., Park, J., Jung, Y., Youn, D. H., Lee, J. H., Jin, J. S., So, H. S., Park, R., Kim, S. H., Kim, S. J., Hong, S. H., and Um, J. Y. (2015) Rubi Fructus (Rubus coreanus) activates the expression of thermogenic genes in vivo and in vitro. *Int. J. Obes. (Lond)* **39**, 456-464
26. Klein, J., Fasshauer, M., Ito, M., Lowell, B. B., Benito, M., and Kahn, C. R. (1999) beta(3)-adrenergic stimulation differentially inhibits insulin signaling and decreases insulin-induced glucose uptake in brown adipocytes. *J. Biol. Chem.* **274**, 34795-34802
27. Yao, H. R., Liu, J., Plumeri, D., Cao, Y. B., He, T., Lin, L., Li, Y., Jiang, Y. Y., Li, J., and Shang, J. (2011) Lipotoxicity in HepG2 cells triggered by free fatty acids. *Am. J. Transl. Res.* **3**, 284-291
28. Kim, H. L., Jeon, Y. D., Park, J., Rim, H. K., Jeong, M. Y., Lim, H., Ko, S. G., Jang, H. J., Lee, B. C., Lee, K. T., Lee, K. M., Lee, H., Kim, S. H., Kim, S. J., Hong, S. H., and Um, J. Y. (2013) Corni Fructus Containing Formulation Attenuates Weight Gain in Mice with Diet-Induced Obesity and Regulates Adipogenesis through AMPK. *Evid. Based Complement. Alternat. Med.* **2013**, 423741
29. Kim, H. L., Sim, J. E., Choi, H. M., Choi, I. Y., Jeong, M. Y., Park, J., Jung, Y., Youn, D. H., Cho, J. H., Kim, J. H., Hwang, M. W., Jin, J. S., Hong, S. H., Cho, H. W., and Um, J. Y. (2014) The AMPK pathway mediates an anti-adipogenic effect of fruits of Hovenia dulcis Thunb. *Food Funct.* **5**, 2961-2968
30. Zhang, C., Chen, D., Liu, X., and Du, l. (2016) Role of brominated diphenyl ether-209 in the proliferation and apoptosis of rat cultured neural stem cells *in vitro Mol. Cell. Toxicol.* **12**, 45-52

31. Youn, D. H., Park, J., Kim, H. L., Jung, Y., Kang, J., Jeong, M. Y., Sethi, G., Seok Ahn, K., and Um, J. Y. (2017) Chrysophanic acid reduces testosterone-induced benign prostatic hyperplasia in rats by suppressing 5alpha-reductase and extracellular signal-regulated kinase. *Oncotarget* **8**, 9500-9512
32. Zhang, Z., Zhang, H., Li, B., Meng, X., Wang, J., Zhang, Y., Yao, S., Ma, Q., Jin, L., Yang, J., Wang, W., and Ning, G. (2014) Berberine activates thermogenesis in white and brown adipose tissue. *Nat. Commun.* **5**, 5493
33. Lee, J. N., Park, J., Kim, S.-G., Kim, M. S., Lim, J.-Y., and Choe, S.-K. (2017) 3-Aminotriazole protects against cobalt (II) chloride-induced cytotoxicity by inhibiting reactive oxygen species formation and preventing mitochondrial damage in HepG2 cells. *Mol. Cell. Toxicol.* **13**, 125-132
34. Martin-Sanz, P., Mayoral, R., Casado, M., and Bosca, L. (2010) COX-2 in liver, from regeneration to hepatocarcinogenesis: what we have learned from animal models? *World J Gastroenterol* **16**, 1430-1435
35. Luedde, T., and Schwabe, R. F. (2011) NF-kappaB in the liver--linking injury, fibrosis and hepatocellular carcinoma. *Nat Rev Gastroenterol Hepatol* **8**, 108-118
36. Tateya, S., Kim, F., and Tamori, Y. (2013) Recent advances in obesity-induced inflammation and insulin resistance. *Front. Endocrinol. (Lausanne)* **4**, 93
37. Leesnitzer, L. M., Parks, D. J., Bledsoe, R. K., Cobb, J. E., Collins, J. L., Consler, T. G., Davis, R. G., Hull-Ryde, E. A., Lenhard, J. M., Patel, L., Plunket, K. D., Shenk, J. L., Stimmel, J. B., Therapontos, C., Willson, T. M., and Blanchard, S. G. (2002) Functional consequences of cysteine modification in the ligand binding sites of peroxisome proliferator activated receptors by GW9662. *Biochemistry* **41**, 6640-6650
38. Aljada, A., Garg, R., Ghanim, H., Mohanty, P., Hamouda, W., Assian, E., and Dandona, P. (2001) Nuclear factor-kappaB suppressive and inhibitor-kappaB stimulatory effects of troglitazone in obese patients with type 2 diabetes: evidence of an antiinflammatory action? *J. Clin. Endocrinol. Metab.* **86**, 3250-3256
39. Brix, J., Dietmeier, K., and Pfanner, N. (1997) Differential recognition of preproteins by the purified cytosolic domains of the mitochondrial import receptors Tom20, Tom22, and Tom70. *J. Biol. Chem.* **272**, 20730-20735
40. Itoh, A., Isoda, K., Kondoh, M., Kawase, M., Kobayashi, M., Tamesada, M., and Yagi, K. (2009) Hepatoprotective effect of syringic acid and vanillic acid on concanavalin a-induced liver injury. *Biol. Pharm. Bull.* **32**, 1215-1219

41. Lemieux, I., Pascot, A., Prud'homme, D., Almeras, N., Bogaty, P., Nadeau, A., Bergeron, J., and Despres, J. P. (2001) Elevated C-reactive protein: another component of the atherothrombotic profile of abdominal obesity. *Arterioscler. Thromb. Vasc. Biol.* **21**, 961-967
42. Rosen, E. D., and Spiegelman, B. M. (2006) Adipocytes as regulators of energy balance and glucose homeostasis. *Nature* **444**, 847-853
43. Gregoire, F. M., Smas, C. M., and Sul, H. S. (1998) Understanding adipocyte differentiation. *Physiol. Rev.* **78**, 783-809
44. Lin, F. T., and Lane, M. D. (1994) CCAAT/enhancer binding protein alpha is sufficient to initiate the 3T3-L1 adipocyte differentiation program. *Proc. Natl. Acad. Sci. U. S. A.* **91**, 8757-8761
45. Farmer, S. R. (2006) Transcriptional control of adipocyte formation. *Cell Metab* **4**, 263-273
46. Polvani, S., Tarocchi, M., Tempesti, S., Bencini, L., and Galli, A. (2016) Peroxisome proliferator activated receptors at the crossroad of obesity, diabetes, and pancreatic cancer. *World J. Gastroenterol.* **22**, 2441-2459
47. Wright, S. K., Wuertz, B. R., Harris, G., Abu Ghazallah, R., Miller, W. A., Gaffney, P. M., and Ondrey, F. G. (2016) Functional activation of PPARgamma in human upper aerodigestive cancer cell lines. *Mol. Carcinog.*
48. Chakrabarti, P. (2010) Promoting adipose specificity: the adiponectin promoter. *Endocrinology* **151**, 2408-2410
49. Tilg, H., and Moschen, A. R. (2006) Adipocytokines: mediators linking adipose tissue, inflammation and immunity. *Nat Rev Immunol* **6**, 772-783
50. Xing, Y., Yan, F., Liu, Y., Liu, Y., and Zhao, Y. (2010) Matrine inhibits 3T3-L1 preadipocyte differentiation associated with suppression of ERK1/2 phosphorylation. *Biochem Biophys Res Commun* **396**, 691-695
51. Tessari, P., Coracina, A., Cosma, A., and Tiengo, A. (2009) Hepatic lipid metabolism and non-alcoholic fatty liver disease. *Nutr. Metab. Cardiovasc. Dis.* **19**, 291-302
52. Rui, L. (2014) Energy metabolism in the liver. *Compr. Physiol.* **4**, 177-197
53. Park, J., and Jang, H.-J. (2017) Anti-diabetic effects of natural products an overview of therapeutic strategies. *Mol. Cell. Toxicol.* **13**, 1-20
54. Feldstein, A. E. (2010) Novel insights into the pathophysiology of nonalcoholic fatty liver disease. *Semin. Liver Dis.* **30**, 391-401

55. Browning, J. D., Szczepaniak, L. S., Dobbins, R., Nuremberg, P., Horton, J. D., Cohen, J. C., Grundy, S. M., and Hobbs, H. H. (2004) Prevalence of hepatic steatosis in an urban population in the United States: impact of ethnicity. *Hepatology* **40**, 1387-1395

56. Hawley, S. A., Boudeau, J., Reid, J. L., Mustard, K. J., Udd, L., Makela, T. P., Alessi, D. R., and Hardie, D. G. (2003) Complexes between the LKB1 tumor suppressor, STRAD alpha/beta and MO25 alpha/beta are upstream kinases in the AMP-activated protein kinase cascade. *J. Biol.* **2**, 28

57. Hurley, R. L., Anderson, K. A., Franzone, J. M., Kemp, B. E., Means, A. R., and Witters, L. A. (2005) The Ca2+/calmodulin-dependent protein kinase kinases are AMP-activated protein kinase kinases. *J. Biol. Chem.* **280**, 29060-29066

58. Sanders, M. J., Grondin, P. O., Hegarty, B. D., Snowden, M. A., and Carling, D. (2007) Investigating the mechanism for AMP activation of the AMP-activated protein kinase cascade. *Biochem. J.* **403**, 139-148

59. Riek, U., Scholz, R., Konarev, P., Rufer, A., Suter, M., Nazabal, A., Ringler, P., Chami, M., Muller, S. A., Neumann, D., Forstner, M., Hennig, M., Zenobi, R., Engel, A., Svergun, D., Schlattner, U., and Wallimann, T. (2008) Structural properties of AMP-activated protein kinase: dimerization, molecular shape, and changes upon ligand binding. *J. Biol. Chem.* **283**, 18331-18343

60. Djouder, N., Tuerk, R. D., Suter, M., Salvioni, P., Thali, R. F., Scholz, R., Vaahtomeri, K., Auchli, Y., Rechsteiner, H., Brunisholz, R. A., Viollet, B., Makela, T. P., Wallimann, T., Neumann, D., and Krek, W. (2010) PKA phosphorylates and inactivates AMPKalpha to promote efficient lipolysis. *EMBO J.* **29**, 469-481

61. Paton, C. M., and Ntambi, J. M. (2009) Biochemical and physiological function of stearoyl-CoA desaturase. *Am. J. Physiol. Endocrinol. Metab.* **297**, E28-37

62. Lopez-Velazquez, J. A., Carrillo-Cordova, L. D., Chavez-Tapia, N. C., Uribe, M., and Mendez-Sanchez, N. (2012) Nuclear receptors in nonalcoholic Fatty liver disease. *J. Lipids* **2012**, 139875

63. Browning, J. D., and Horton, J. D. (2004) Molecular mediators of hepatic steatosis and liver injury. *J. Clin. Invest.* **114**, 147-152

64. Andreelli, F., Foretz, M., Knauf, C., Cani, P. D., Perrin, C., Iglesias, M. A., Pillot, B., Bado, A., Tronche, F., Mithieux, G., Vaulont, S., Burcelin, R., and Viollet, B. (2006) Liver adenosine monophosphate-activated kinase-alpha2 catalytic subunit is a key

target for the control of hepatic glucose production by adiponectin and leptin but not insulin. *Endocrinology* **147**, 2432-2441

65. Merrill, G. F., Kurth, E. J., Hardie, D. G., and Winder, W. W. (1997) AICA riboside increases AMP-activated protein kinase, fatty acid oxidation, and glucose uptake in rat muscle. *Am. J. Physiol.* **273**, E1107-1112

66. Jager, S., Handschin, C., St-Pierre, J., and Spiegelman, B. M. (2007) AMP-activated protein kinase (AMPK) action in skeletal muscle via direct phosphorylation of PGC-1alpha. *Proc. Natl. Acad. Sci. U. S. A.* **104**, 12017-12022

67. Canto, C., Gerhart-Hines, Z., Feige, J. N., Lagouge, M., Noriega, L., Milne, J. C., Elliott, P. J., Puigserver, P., and Auwerx, J. (2009) AMPK regulates energy expenditure by modulating NAD+ metabolism and SIRT1 activity. *Nature* **458**, 1056-1060

68. Fenzl, A., and Kiefer, F. W. (2014) Brown adipose tissue and thermogenesis. *Horm. Mol. Biol. Clin. Investig.* **19**, 25-37

69. Palou, A., Pico, C., Bonet, M. L., and Oliver, P. (1998) The uncoupling protein, thermogenin. *Int. J. Biochem. Cell Biol.* **30**, 7-11

70. Brondani, L. A., Assmann, T. S., Duarte, G. C., Gross, J. L., Canani, L. H., and Crispim, D. (2012) The role of the uncoupling protein 1 (UCP1) on the development of obesity and type 2 diabetes mellitus. *Arq. Bras. Endocrinol. Metabol.* **56**, 215-225

71. Ouellet, V., Labbe, S. M., Blondin, D. P., Phoenix, S., Guerin, B., Haman, F., Turcotte, E. E., Richard, D., and Carpentier, A. C. (2012) Brown adipose tissue oxidative metabolism contributes to energy expenditure during acute cold exposure in humans. *J. Clin. Invest.* **122**, 545-552

72. Crowley, V. E., Yeo, G. S., and O'Rahilly, S. (2002) Obesity therapy: altering the energy intake-and-expenditure balance sheet. *Nat. Rev. Drug Discov.* **1**, 276-286

73. Baumruk, F., Flachs, P., Horakova, M., Floryk, D., and Kopecky, J. (1999) Transgenic UCP1 in white adipocytes modulates mitochondrial membrane potential. *FEBS Lett.* **444**, 206-210

국문 초록

바닐릭 산의 AMPK 기전 및 열 생성 조절 인자를 통한 항비만 효과에 대한 연구

정윤우

경희대학교 대학원

지도교수: 엄재영

비만을 비롯한 대사질환은 전세계의 건강문제로 대두되고 있다. 현행 비만치료제가 부작용 등으로 인한 한계점에 봉착함에 따라, 상대적으로 부작용이 적은 천연물을 대상으로 신규 항비만 소재의 개발에 대한 연구가 진행되고 있으며, 특히 AMP-activated protein kinase (AMPK)와 비떨림 열생성 기전을 통한 에너지대사의 활성화는 비만 치료의 신규한 타겟으로 주목받고 있다. 따라서, 본 연구는 바닐릭 산의 항비만 효과를 확인함과 동시에 AMPK 기전 및 열 생성 인자에 대한 바닐릭 산의 상세 조절 기전을 규명하기 위해 진행되었다.

고지방식이 유도 비만 C57BL6 마우스와 렙틴 수용체의 유전적 결핍으로 인해 비만 형질을 나타내는 *Lepr*$^{-/-}$ (*db/db*) 마우스를 활용한 생체 내 실험에서 바닐릭 산의 투여에 의해 체중 및 조직 무게가 유의적으로 감소되었으며, 특히 대사와 관련된 기관인 백색지방, 갈색지방, 간 조직에서 AMPK 기전이 활성화되었다. 또한, HepG2 간 세포, 3T3-L1 지방세포, 일차배양 갈색지방세포를 이용한 생체 외 연구에서 바닐릭 산의 처리는 HepG2 세포의 지방 축적 및 염증 관련 인자를 감소시키는 한 편, AMPK 와 미토콘드리아 대사 인자를 포함한 에너지 대사 관련 인자의 증가를 유도했으며, 3T3-L1 백색지방세포에서 역시 유의적인 지방 축적의 감소와 함께 PPARγ 와 C/EBPα 를 비롯한 분화 관련 인자의 감소 및 AMPK 기전의 활성화를 유도하였다. AMPK 에 대한 siRNA 처리와 AMPK 억제제인 compound C 처리를 통해 바닐릭 산의 상세 작용 기전을 확인한 결과, AMPK 가 차단된 환경에서는 바닐릭 산의 효과가 반감되었다. 또한, 일차배양 갈색지방

세포에서 바닐릭 산은 미토콘드리아의 발열 관련 인자인 UCP1 과 PGC1α 등을 활성화시켰다.

본 연구는 바닐릭 산이 AMPK 의 활성화 및 열 발생 작용을 통해 지방 축적을 억제하고 에너지 대사를 증가시킴으로써 항비만 효과를 가짐을 보여주며, 이러한 결과는 바닐릭 산의 새로운 기전의 신규 항비만 치료제로서의 가능성을 시사한다.

핵심어: vanillic acid; obesity; adipogenesis; thermogenesis; AMP-activated protein kinase alpha